European Review for Medical and Pharmacological Sciences 2023; 27: 7201-7225

# Diagnostic approach to focal liver lesions at cross-sectional imaging: a primer for beginners

A. BORGHERESI[1], A. AGOSTINI[1,2], L. PIERPAOLI[3], A. ZANNOTTI[3], S. CAPODAGLI-COLARIZI[3], M. GABELLONI[4], F. DE MUZIO[5], M.C. BRUNESE[5], F. BRUNO[2,6], P. PALUMBO[2,6], F. GRASSI[7], R. FUSCO[8], V. GRANATA[9], N. GANDOLFO[10], V. MIELE[2,11], A. BARILE[12], A. GIOVAGNONI[1]

[1]Department of Clinical, Special and Dental Sciences, University Politecnica delle Marche, Department of Radiological Sciences, University Hospital "Azienda Ospedaliero Universitaria delle Marche", Ancona, Italy
[2]Italian Society of Medical and Interventional Radiology (SIRM), SIRM Foundation, Milan, Italy
[3]School of Radiology, University Politecnica delle Marche, Ancona, Italy
[4]Department of Translational Research, Nuclear Medicine Unit, University of Pisa, Pisa, Italy
[5]Department of Medicine and Health Sciences V. Tiberio, University of Molise, Campobasso, Italy
[6]Department of Diagnostic Imaging, Area of Cardiovascular and Interventional Imaging, Abruzzo Health Unit 1, L'Aquila, Italy
[7]Department of Precision Medicine, Università degli Studi della Campania "Luigi Vanvitelli", Naples, Italy
[8]Medical Oncology Division, Igea SpA, Naples, Italy
[9]Division of Radiology, Istituto Nazionale Tumori IRCCS Fondazione Pascale–IRCCS di Napoli, Naples, Italy
[10]Diagnostic Imaging Department, Villa Scassi Hospital–ASL 3, Genoa, Italy
[11]Department of Radiology, Azienda Ospedaliero-Universitaria Careggi, Florence, Italy
[12]Department of Biotechnological and Applied Clinical Sciences, University of L'Aquila, L'Aquila, Italy

**Abstract. – Liver imaging encompasses a broad spectrum of diseases in different clinical backgrounds. The available literature is vast and reported data often lacks standardization. Because of all these issues, the differential diagnosis and the characterization of liver lesions can be challenging for the beginner. The aim of this narrative review is to provide the basics for an algorithm approach to liver lesions on cross-sectional imaging. First, some tips for the optimization of Computed Tomography (CT) and Magnetic Resonance Imaging (MRI) protocols will be provided. Liver Imaging Reporting and Data System (LI-RADS, version 2018) working group is proposing the adoption of their standardized lexicon beyond the original target population of LI-RADS (i.e., liver cirrhosis). Thus, the main imaging findings will be defined following the LI-RADS lexicon. Since the contrast study is the most important for lesion characterization, this narrative review separates the lesions into avascular, hypovascular, and hypervascular, with a focus on chronic liver disease (CLD) and hepatocellular carcinoma (HCC).**

*Key Words:*
Liver, Liver lesion, Computer assisted tomography, Magnetic resonance imaging, Hepatocellular carcinoma, Cholangiocellular carcinoma, Metastasis, Focal nodular hyperplasia, Hepatocellular Adenoma, Hepatic Hemangioma, Liver Imaging Reporting and data system, LI-RADS.

## Introduction

The detection of an incidental liver lesion is becoming increasingly frequent thanks to technological advances and the widespread use of cross-sectional imaging[1,2]. Accurate characterization is fundamental to avoid unnecessary, invasive, and potentially harmful procedures[3]. Differential diagnosis may be challenging for the beginner due to the wide spectrum of disease, the overlap of imaging findings, and the need for integration with the clinical background[1,3].

The published literature on the characterization of liver lesions at cross-sectional imaging is huge, and it can be difficult to be summarized due to the variability in lexicon and definitions[4]. Among liver lesions, the radiological features of hepatocellular carcinoma (HCC) have been

*Corresponding Author:* Andrea Agostini, MD; e-mail: dott.andrea.agostini@gmail.com

standardized, and the diagnosis can be placed only on the imaging findings[5,6]. The standardization of the radiological lexicon is one of the main aims of the Liver Imaging Reporting and Data System (LI-RADS)[7]. Knowing the advantages and the increasing diffusion of the standardized assessment of imaging findings in different fields, the LI-RADS Commission is pushing the adoption of the lexicon beyond the cirrhotic condition[7-9].

Different LI-RADS criteria have been developed for ultrasound (US), computed tomography (CT) and magnetic resonance imaging (MRI)[10]. However, multiphasic contrast-enhanced CT and MRI remain the cornerstone for the characterization of liver lesions in all clinical scenarios[11].

This narrative review starts with an overview of the optimization of CT and MRI protocols in liver imaging will be provided. Then, some clarifications about the LI-RADS standardized lexicon will be discussed. Therefore, the liver lesions will be divided into avascular, hypovascular, and hypervascular, in cirrhotic and non-cirrhotic liver to describe an algorithmic approach to their differential diagnosis.

## The Basics: Proper CT and MRI Techniques

### CT

Multi-detector CT (MDCT) is usually the first examination performed for the evaluation of a liver lesion; therefore, it is important to implement the appropriate protocol to achieve the best diagnostic result[12]. An inadequate examination would strongly affect the possibility of placing the right diagnosis.

The standard liver protocol usually includes a pre-contrast (basal) acquisition, even if, in some cases, it is considered optional. Specifically, the basal scan is used to detect the presence of blood, fat, proteinaceous material, or hyperdense remnants (e.g., iodized oil) from the previous treatments[10]. Also, the accuracy of the measurements of liver metastases and the assessment of pseudolesions or lesions with faint enhancement is significantly improved when the basal acquisition is used as reference[13-15].

The basal acquisition is followed by the multiphasic, post-contrast study, with an arterial phase (AP), a portal venous phase (PVP), and a delayed phase (DP). The AP highlights hypervascular lesions against the poorly enhanced liver parenchyma and classified as "early" or "late". The "early" AP is characterized by the enhancement of the hepatic artery without significant enhancement of the portal vein nor the liver parenchyma. Conversely, the "late" AP is considered optimal when the arterial enhancement of the hepatic parenchyma, the initial enhancement of the portal vein without forward enhancement of the hepatic veins, are present[10]. Some liver lesions can be missed at the "early" AP, so the "late" AP is considered the most accurate for the detection of hypervascular liver lesions[16,17]. Since the time window of the "late" AP is relatively narrow, protocols including bolus tracking or test bolus techniques are warranted[18]. If the bolus tracking technique is used, the "late" AP is typically acquired with a delay of 10-30s after the aortic threshold of 100-150 HU. For the test bolus, 10-20s after the aortic peak are considered acceptable[19]. A more detailed description is provided in Bae et al[18].

The PVP has a wider time window, between 60s to 90s after the start of the injection of the contrast material (CM). It provides the optimal enhancement of liver parenchyma and its vascular structures[20]. For these reasons, PVP is the most reliable phase for the evaluation of hypovascular lesions (e.g., metastases), wash-out, residual enhancement of HCC, biliary abnormalities, or intrahepatic vessels[19,21].

The DP is usually acquired at 3-5 min; it was previously known as the "equilibrium" phase. As the name suggest, in this phase the CM is substantially "equilibrated" across the vascular and the interstitial compartments[19]. This is helpful for the assessment of hypovascular tumors and wash-out[19,22,23].

Two principles must be considered for the optimization of the CM in liver studies. First, the arterial phase is more dependent on the cardiac output and iodine delivery rate (given by the concentration and the injection rate of the CM). Second, the optimal enhancement of the liver parenchyma during the portal phase (≥50HU) requires a dose of contrast material tailored to the anthropometric data[18,19,24-28].

The radiation dose is another aspect to be considered in the optimization of the CT protocol[29,30]. The technological advances in tubes and detectors allow for the routinary acquisitions at low kV, with a significant reduction in radiation dose and iodine load, with better contrast of liver lesions[31-34]. In this scenario, the image quality can be further improved by the introduction of Iterative Reconstruction (IR). The advantages of IR in terms of dose re-

duction, image quality and noise, and conspicuity of liver lesions have been proven[35-37]. However, the specific limitations of IR in liver imaging must be addressed for their optimal use[36,38]. More recently, deep-learning reconstructions have been developed to overcome the limitations of IR[39,40]. Material decomposition on Dual-energy CT (DECT) opens new perspectives on CT imaging[41]. Specifically, virtual unenhanced images form DECT datasets that have the potential for dose reduction by avoiding basal acquisitions[41]. Virtual monochromatic images can be used for contrast optimization and iodine maps that may be helpful for a better lesion characterization[42,43].

### *MRI*

Magnetic Resonance imaging (MRI) provides a comprehensive, multiparametric assessment of the liver; therefore, it is considered a problem-solving technique[44]. The standard protocol for the liver study relies on T1, T2, diffusion-weighted images (DWI), and the post-contrast study[45,46]. The advanced techniques, such as fat and iron quantification, and MRI perfusion, are beyond the scope of this paper and are exposed elsewhere[44,45].

The examination usually starts with a Single Shot Fast Spin Echo (SSFSE), T2w sequence on the coronal plane: it provides a fast, general overview of the upper abdomen with acceptable image quality[47.] The protocol continues with axial, usually Fast Spin Echo (FSE) or SSFSE, moderately T2 weighted (w) images (optimal echo time, TE, 80-100ms). Two main points must be discussed. First, the FSE sequences are prone to J-coupling with abnormal hyperintensity of fat, so fat saturation is necessary[48]; the preferred techniques are spectral fat saturation or inversion recovery techniques[44,46]. Second, some authors suggested to both acquire moderately and heavy T2w images (TE>160 ms). This would allow a more accurate differentiation of benign and cystic-like lesions (which maintain the hyperintensity), from "solid" lesions (more hypointense at longer TE)[49,50].

For T1 images, Gradient Recalled Echo (GRE) sequences are used[51]. These images are useful to assess substances with high signal on T1 images, such as fat, hemorrhage, protein materials, or glycogen[52,53]. Moreover, GRE sequences are sensitive to susceptibility artifacts, optimal for the detection of metals (such as iron compounds), calcium, and air[44,46]. In the basic protocol, the dual-echo GRE has the echo times set at phase coherence and opposition of fat and water signals[45]. Conventionally, to distinguish and reduce the T2* effect while assessing steatosis, the out-phase (OP) images have shorter TE than the in-phase (IP)[52]. More recently, 3D sequences, and Dixon techniques for optimal water/fat separation, are increasingly used[52,54].

The DWI evaluates the Brownian motion of the water molecules; several different models have been developed to assess tumor cellularity[55-57]. DWI has a relevant role for lesion detection, with higher conspicuity and better detection of subcentimetric lesions[58,59]. The data regarding DWI for lesion characterization are encouraging, but the effectiveness is still limited[58-61]. Eco Planar Imaging (EPI) is routinely used in the liver protocol, with different b values to assess the water diffusivity[62]. The basic protocol must contain at least one series with b<100 to obtain T2w images with black blood and acceptable signal-to-noise and contrast-to-noise ratios (SNR and CNR), and further series high b-values (typically b=800-1,000 s/mm$^2$)[62,63]. The interpretation of DWI can be qualitative or quantitative. Since tissues with T2 signal may be misleadingly bright on DWI with high b-values (i.e., T2 shine-through artifact), the combined evaluation with the Apparent Diffusion Coefficient (ADC) maps avoids misdiagnoses[45,62]. Conversely, the significant overlap of ADC values of the different lesions limits the application of quantitative methods for lesion characterization[45,62,63].

Similarly to CT, the post-contrast study is necessary for accurate lesion detection and characterization. Rapid, spoiled T1w 3D GRE sequences with a high temporal resolution are used[54,64]. Pre-contrast series are acquired for subtraction and basal assessment[45]. The acquisition times of post-contrast phases reflect the principles discussed for CT but consider the filling mode of the k-space[20,44-46,65]. The CM routinely administered are Gd-chelates with vascular-interstitial kinetics, except for two (Gd-BOPTA and Gd-EOB-DTPA) which are actively assimilated by the hepatocytes in variable proportions[66,67]. The hepatospecific contrast agents (HSCA) have several advantages: they provide metabolic information about the hepatocytes and lesions, improve lesion detection and conspicuity, and allow the assessment of the biliary tree[68-74]. However, their use requires adjustments in protocols (e.g., longer acquisition times) and in image interpretation[45,67]. Since Gd-EOB-DTPA is characterized by an early uptake, the lesion washout can be assessed only on the PVP, and the delayed phase cannot be named "equilibrium" phase but "transitional" phase[75].

## The Basics: Some Considerations About Liver Parenchyma and Prevalence of Liver Lesions

The American College of Radiology (ACR) defines the focal liver lesion detected during an examination for unrelated reasons as "incidental"[3]. The accurate characterization of the finding is fundamental for the adequate management. The assessment starts from the clinical background[3].

Several clinical conditions influence the prevalence of focal liver lesions in adult patients[3,76]. Karhunen et al[77] evaluated an autoptic case series of 95 adult men dead of cardiovascular accidents or violent death. The authors found a liver lesion in 49 (52%) of cases: 26 subjects (27%) had benign lesions of the bile ducts (hamartomas or adenomas), 19 (20%) had hepatic hemangiomas (HH), and 3 (3%) subjects had focal nodular hyperplasia (FNH)[77]. Other lesions were rare: (1%) case of hepatocellular adenoma (HA), 1 (1%) case of nodular regenerative hyperplasia, 1 (1%) subject with peliosis, and 1 (1%) with colorectal liver metastases[77]. The lesions were globally small (the mean diameters ranged from 1.3 mm of the biliary lesions to 8 mm of the FNH), the prevalence increased with age, and in at least 40% of cases, were multiple[77]. This trend is confirmed by ultrasound (US) studies[78,79] in large populations. Kaltenbach et al[78] presented similar US findings on 45,319 patients. They recorded 2,839 focal fatty changes (6.26%), 2,631 (5.81%) cysts, 1,640 (3.62%) HH, 81 (0.18%) FNH, and 19 (0.04%) HA. Oshibuchi et al[79] reported similar findings in a previous study on a smaller population.

The circumstances are different for symptomatic or oncological patients. Although most of the liver lesions radiologically detected in this setting are benign (up to 80%-92%), metastases have a significant prevalence (nearly 4-22%)[80-83]. These findings are comparable to the autoptic case series of Ono et al[84]: they found liver metastases in 38 cases (27%) in 142 patients with urologic malignancies.

Liver cirrhosis represents another different scenario. Here, regenerative-dysplastic and HCC nodules are the most frequent findings, with an incidence rate of up to 6/100,000 per year[5]. Dodd et al[85,86] reported the imaging and pathological findings in 508 explanted cirrhotic livers. The authors found dysplastic nodules in 57 (11%) of livers and HCC in 46 (9%) livers[86]. Caroli-Bottino et al[87] evaluated 30 explanted cirrhotic livers. In 11/30 (36.7%) cases, there was a known radiological diagnosis, while in the remaining 19/30 (63.3%), there was an incidental detection of HCC – all livers had at least 1 HCC[87]. Regarding benign lesions, Dodd et al[86] found only 9 HH (1.8%) in their case series. Moreover, the occurrence of liver metastases in oncological patients with cirrhosis is lower (23.7% *vs.* 37.3% in the metanalysis of Seymour et al[88]).

In conclusion, a liver lesion should be evaluated first on the basis of the patient risk profile, i.e., healthy subjects, patients with known malignancy, and chronic liver disease. The ACR white paper on incidental liver lesions defines a "high-risk category" including the latter two conditions[3]; another useful classification is based only on the presence or absence of chronic liver disease.

## Characterization of Liver Lesions: Main Findings, Lexicon, and Standardization

The groundwork for an accurate characterization of a liver lesion relies on univocal definitions of the observed findings. This allows a concise and precise report (eventually a structured report), ensuring the correct communication with other specialists[4,89-93]. However, the available radiological literature on liver lesions is vast, and incongruences in terms and definitions are widespread. As an example, arterial phase hyperenhancement (APHE) of HCC is defined as "arterial enhancement" in Freeman et al[94], "arterial wash-in" in a version of the Latin American for the Study of the Liver (LAASL) guidelines[95], and as "hypervascularization", "arterial-phase hypervascularity", or "arterial-phase enhancement" in Bolondi et al[96].

The LI-RADS criteria (updated in 2018) by the ACR, aims to provide a diagnostic algorithm for the radiological diagnosis of HCC in at-risk[4,7,10]. The Committee also provides a standardized, comprehensive lexicon to improve the image interpretation, even in less-experienced readers, with beneficial effects on clinical communication, education and research[7,97-101]. The LI-RADS lexicon was further upgraded in 2021[102]. In this version, the Working Group provides the Context of Use of each term (namely "Broad" or "Restricted to LI-RADS" target populations) with the aim to expand the utilization beyond cirrhotic patients[9,102,103]. Interestingly, 69 of 81 terms defined are applicable in the broad scenario[9,103].

In this context, it is worth summarizing the main definitions to provide a framework for the assessment of a liver lesion. First, a focal abnormality in the liver is hierarchically defined as an observation. This can be considered as a lesion if it corresponds

to a pathological abnormality, while, if not, it is a pseudo lesion[104]. If the lesion is <2 cm, it is a nodule. If the lesion causes distortion/destruction of anatomical structures, it is defined as a mass, otherwise, it is a nonmass-like lesion[4,9,102,105].

The characterization of a liver lesion considers the features at basal acquisitions paired with the behavior after CM injection. While basal acquisition in CT provides limited information, lesion characterization on MRI starts with the assessment of basal T2w, T1w, and DWI images[11]. The qualitative assessment signal of liver lesions on T1w and T2w images derives from the early investigations showing altered relaxation times of neoplastic nodules[106]. The most accepted biological model involves the differences in the interactions between water and macromolecules in normal or pathological tissues, leading to the typical signal characteristics on T1w and T2w images[107-109].

The LI-RADS system distinguishes the mild-moderate and the marked T2 hyperintensity[9,102,109]. In the first case, the lesion is mildly hyperintense than the liver on T2w images, with a signal similar to the spleen. This is suggestive of general malignancy, but it can be noticed also in benign lesions (Figure 1)[109-112]. Conversely, a markedly T2 hyperintense lesion (Figure 2) has a signal intensity similar to static fluids (eventually maintained at longer echo times); it is suggestive of benignity, with the exception of cystic or hypervascular malignancies[109,113,114].

The next sequence to be evaluated is the DWI. In the LI-RADS lexicon, the restricted diffusion is defined as the combination of hyperintensity of the observation at medium-high b values (≥400 s/mm$^2$) together with a signal lower than the liver on the ADC map. The consensual assessment of the two images is strongly recommended to avoid the T2 shine-through artifact (Figure 2)[109]. In general, the biological basis of restricted diffusion relies on multiple, complex factors leading to the limitation of the Brownian motions of the water molecules in the neoplastic tissues compared to the normal ones[57,63]. The LI-RADS system includes the

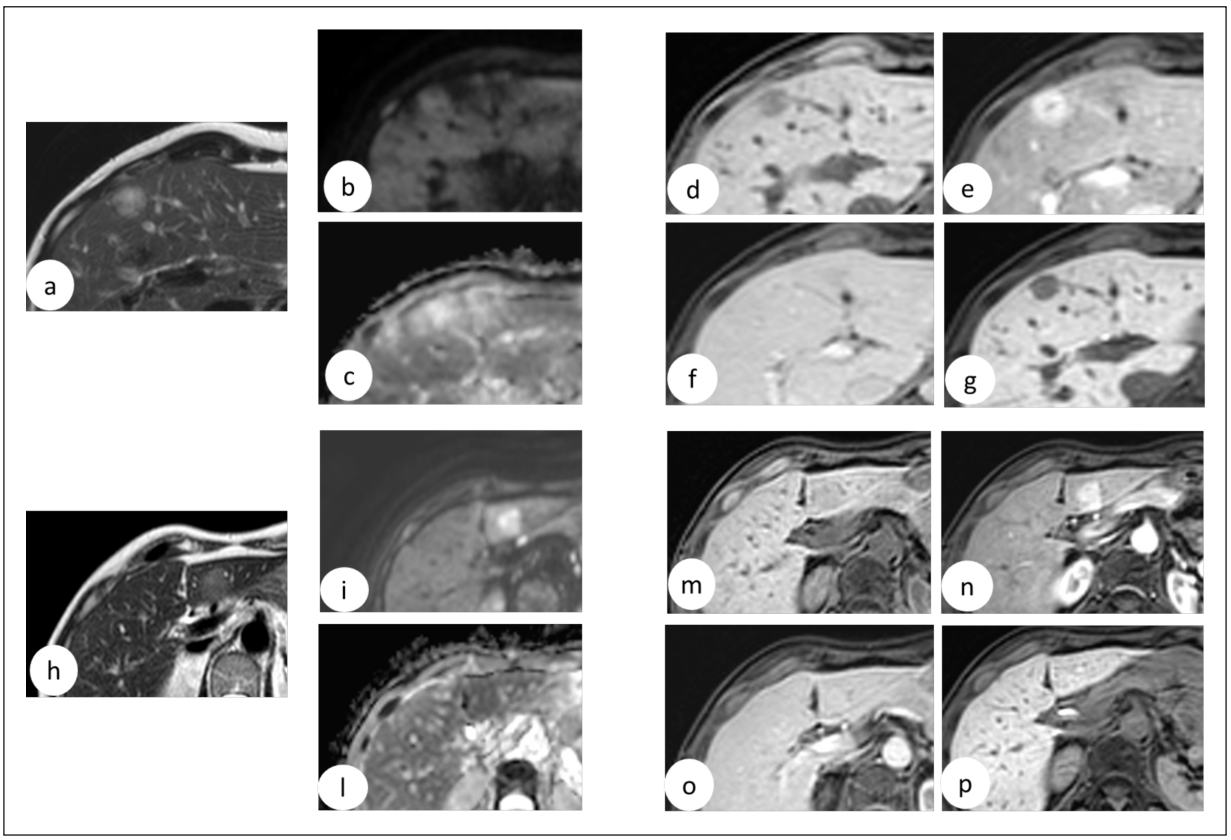


**Figure 1.** Hepatocellular Adenoma (HA, **a-g**) and Focal Nodular Hyperplasia (FNH, **h-p**) on MRI with gadoxetic acid. **a,h**, T2w images. **b,i**, DWI b=800 s/mm$^2$; (**c,l**) ADC map (mm$^2$/s). **d-g, - m-p**, 3D GRE, fat-suppressed, T1w images. Contrast study: basal, (**m**), late arterial (**e,n**), portal venous (f,o), and hepatobiliary phases (**g,p**). Images show lesions with *mild-moderate hyperintensity* on T2w images, with variable restriction on DWI-ADC images, *nonrim APHE*, with hypointensity (HA), (**g**) and iso-hyperintensity (FNH), (**p**) on the hepatobiliary phase.

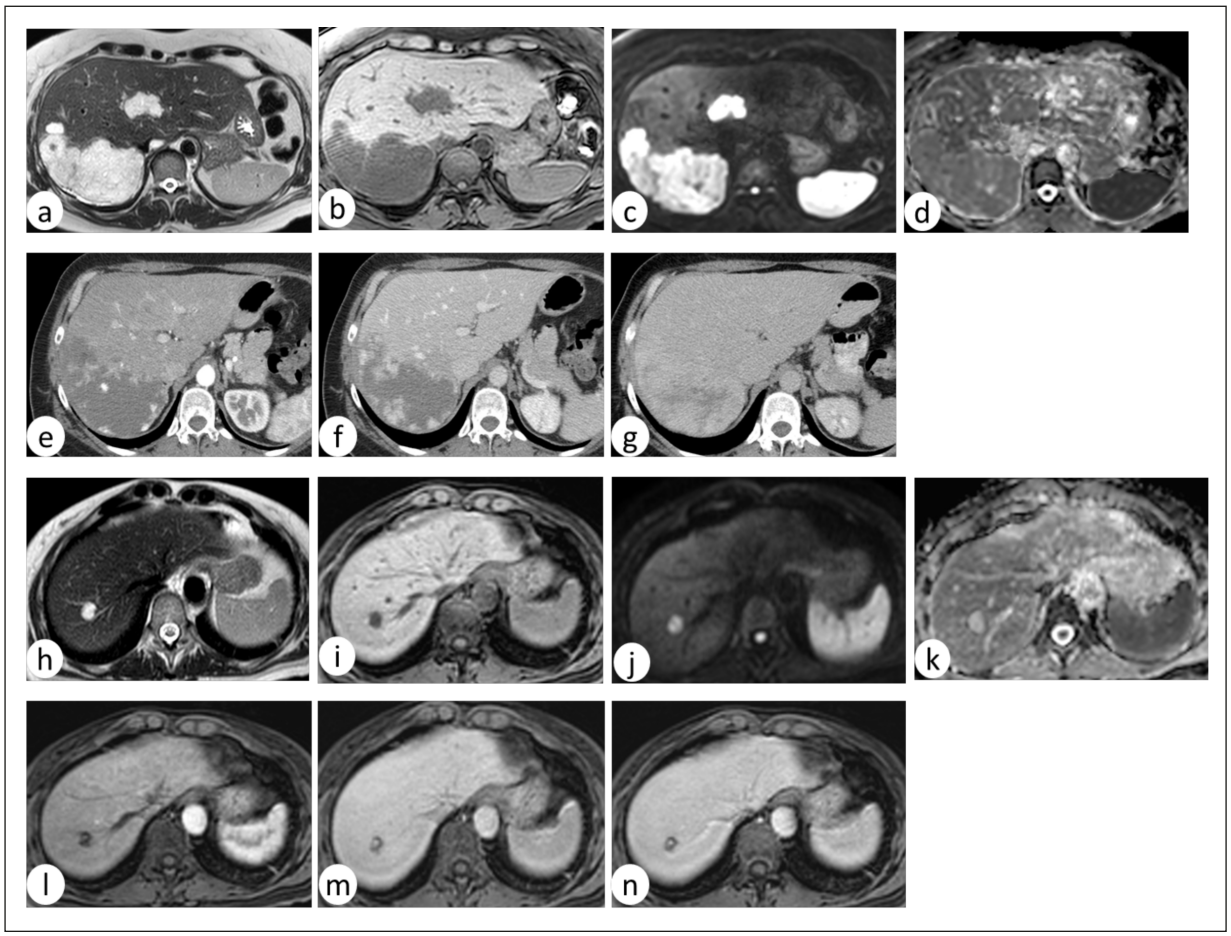


***Figure 2.*** Hepatic Hemangioma (HH). **a-g**, Giant cavernous HH. (h-n) small, typical HH. (**a,h**) T2w images; (**b,i**) 3D GRE, fat-suppressed, T1w images; (**c,j**) DWI b=800 s/mm$^2$; (**d,k**) ADC map (mm$^2$/s). **e-g**, contrast-enhanced CT (late arterial, portal, venous phase). **l-n**, contrast-enhanced MRI with 3D GRE, fat-suppressed, T1w images (late arterial, portal, venous phase). Lesions show the typical marked T2 hyperintensity and hypointensity on T1w images. The consensual assessment of DWI and ADC maps allow to avoid the T2 shine-through effect visible as hyperintensity on b800. The contrast studies show peripheral nodular enhancement, which is comparable to the vascular compartment (*parallels blood pool enhancement*).

DWI-ADC among the imaging features suggestive of malignancy; it distinguishes a nontargetoid and a targetoid restricted diffusion[102,109]. A qualitative, visual assessment of the images is recommended, and a marked or mild restriction are distinguished[102,109]. It is acknowledged that DWI-ADC has a lower sensitivity for HCC than for other malignancies, due to several factors (e.g., differentiation)[115].

A difference in fat or iron content between a lesion and the surrounding liver is helpful for the characterization. A lower intralesional fat content than the surrounding liver is suspicious of any malignancy, while a higher intralesional fat suggests the hepatocellular origin of the lesions, which can be malignant or benign[109,116]. On CT, a lesion with increased fat is significantly hypoattenuating (<10 HU) if compared to a less or non-steatotic liver. Conversely, a hyperattenuating lesion, more than a steatotic, surrounding liver (liver attenuation ≤40 HU) has a reduced fat content[109]. On MRI, the differences in fat content between the lesion and the liver are assessed by the signal decay on the in-phase images or on the fat-only of fat-fraction maps[109]. The iron content is preferably assessed on MR[109]. While the increased intralesional iron suggests benignity (e.g., dysplastic nodules in chronic liver disease), reduced iron content is suggestive of a malignant lesion[109]. The effects of iron on T2* relaxation causes signal decay in the sequences with long echo times (i.e., hypointensity on T2w sequences or signal decay on out-phase images) or on R2* maps[6,109,117,118].

The assessment of the contrast study is fundamental for the differential diagnosis of a liver lesion. In general, liver lesions are characterized by assessing the contrast enhancement at specific

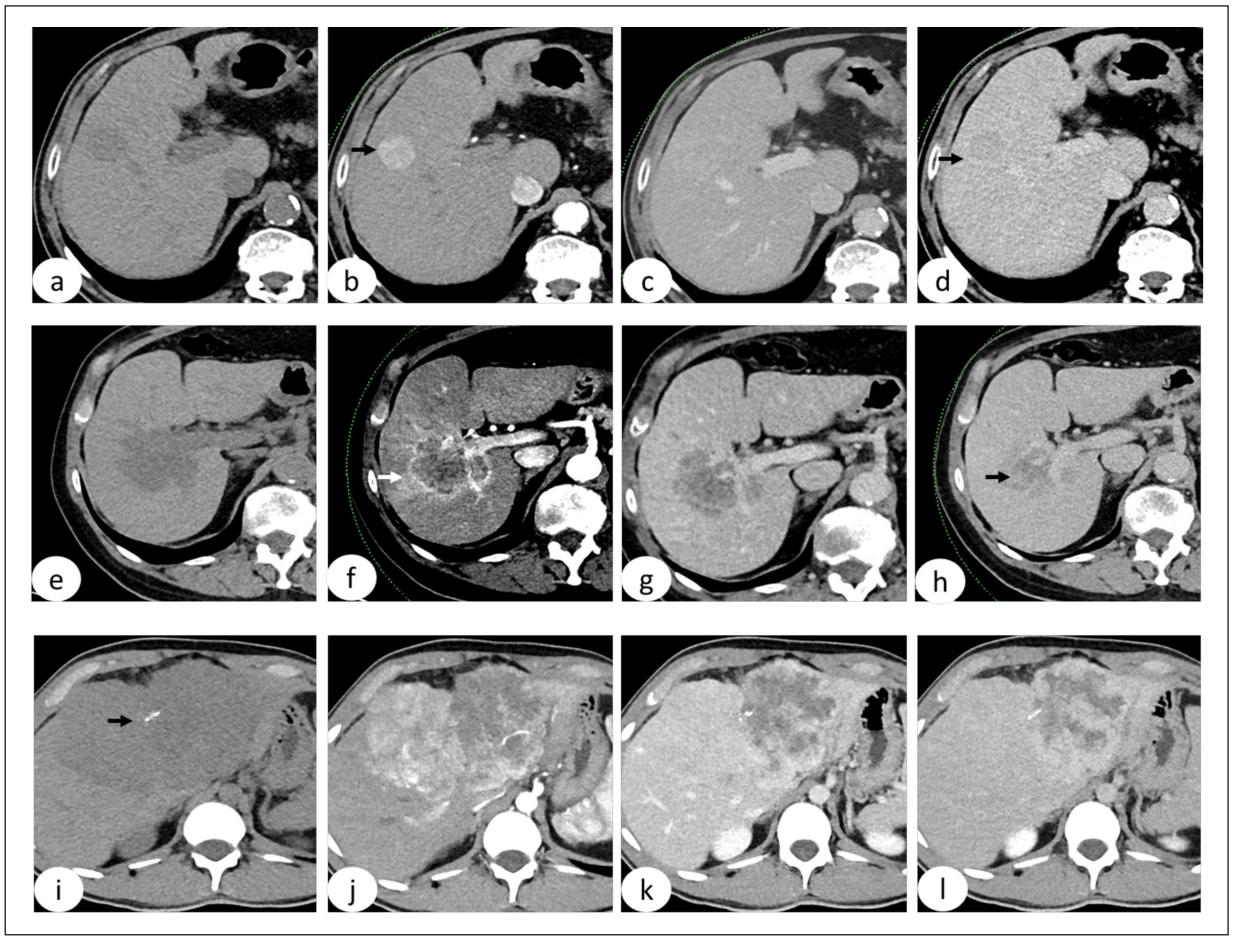


**Figure 3.** Hepatocellular Carcinoma [HCC, (**a-d**)], Intrahepatic Cholangiocellular Carcinoma [iCCC, (**e-h**)], Fibrolamellar HCC on CT (**i-l**). **a,e,i**, Basal acquisition, (**b,f,j**) late arterial, (**c,g,k**) portal venous, **d,h,l**: late phases. HCC shows the typical *nonrim APHE* [arrow in (**b**)], with *washout* on the late phase [arrow in **d**). iCCC shows the *rim APHE* [arrow in (**f**)] with a delayed enhancement of the central fibrous component [arrow in (**h**)], describing a *targetoid appearance*. Fibrolamellar HCC shows calcification at basal acquisition [arrow in (**i**)], with heterogeneous APHE and washout (**j-l**).

time points after the injection, i.e., the post-contrast phases already described[109]. First, there is Arterial phase enhancement (APHE), when the enhancement of the lesion is higher than the surrounding liver either during the early or late AP. However, as previously mentioned, APHE can be confidently assessed on the late AP independently from the findings on the early AP[16,109]. Therefore, the late AP is crucial for the contrast study of the liver. In fact, the APHE cannot be excluded if it is absent on the early AP. Moreover, if the early AP is the only available AP and the APHE is absent, this finding must be considered as non-characterizable[109]. Two subcategories of APHE are identified into the LI-RADS system: the nonrim and the rim APHE. The first reflects a diffuse arterial blood supply of the lesion, which can be considered as benign or malignant (i.e., the gradual, diffuse neoangiogenesis of the HCC) (Figure 1; Figure 3). Conversely, the rim APHE is a sign of neoangiogenesis at the tumor periphery, which is typical of other malignancies, such as intrahepatic (i) cholangiocellular carcinoma (CCC) (Figure 3)[109,119].

The term washout describes the temporal reduction of the contrast enhancement after the AP: the lesion shows a hypoenhancement relative to the surrounding liver parenchyma in the PVP and/or the DP (Figure 3)[109,120]. The washout has two subtypes related to its spatial distribution within the lesion: if more prominent at the periphery of the lesion, it is peripheral; otherwise, it is nonperipheral. Like rim APHE, the peripheral washout can be observed in non-HCC malignancies with the neoplastic cellular component at the periphery, such as iCCC (Figure 3)[109]. It must be pointed out that the progressive reduction of

the enhancement resulting in isointensity of the observation with the surrounding liver is not considered wash-out but fade[109].

Other contrast behaviors suggestive of benignity are defined in the LI-RADS system[109,121]. The parallels blood pool enhancement and peripheral discontinuous nodular enhancement are patterns suggestive of Hepatic Hemangioma (HH)[122]. In the first, the lesion contrast enhancement mirrors the blood pool (i.e., arteries or veins depending on the phase); in the second case, the lesion has peripheral, expanding areas of enhancement mirroring the blood compartment (Figure 2)[122,123].

The contrast study involves the assessment of the transitional and hepatobiliary phases after HSCA. While the isointensity or faint hypointensity are suggestive of hepatocellular, benign lesions or pseudolesions, the hypointensity is suggestive of a malignant or non-hepatocellular lesion (Figure 1)[68,124-126].

In LI-RADS version 2018, the capsule has a context of use limited to chronic liver disease[102]. It refers to a smooth, sharp border around an observation that is more conspicuous than the fibrotic tissue surrounding the cirrhotic nodules. The radiological term capsule refers either to a true capsule (i.e., confirmed at pathology) or to a pseudocapsule (i.e., without correspondence at pathology)[109]. These two entities cannot be distinguished at imaging. The presence of a capsule is mostly associated to HCC; conversely, other malignancies, such as iCCC, have more infiltrative growth. The LI-RADS identifies two subcategories: enhancing and nonenhancing capsule. Specifically, the enhancing capsule is visible as an enhancing rim in the post-arterial phases (except for the hepatobiliary phase) and is a characteristic sign of progressed HCC[109].

All the features described with a concentric pattern are globally encompassed within the targetoid appearance. It is defined when at least one of the following features are present: the rim APHE, the peripheral washout, the delayed central enhancement, the targetoid appearance in the transitional or hepatobiliary phase, and the targetoid diffusion restriction. These features are included into the LI-RADS M category (i.e., high probability of malignancy but not specific for HCC)[6]. These findings are generally referred to other malignancies than HCC, such as iCCC (Figure 3), where the neoplastic cellular component is in the periphery and the core is fibrotic, ischemic or necrotic[109,127,128]. However, it must be considered that a small percentage of HCC can show these features. Moreover, other non-neoplastic conditions may have (e.g., abscesses) or may simulate these features (e.g., granulation tissue after locoregional treatments)[109].

## Avascular Lesions: an Algorithmic Approach to Hepatic Cystic Lesions

Hepatic cysts (HC) are fluid-filled lesions with or without an epithelial layer and represent a frequent, often incidental finding[78,129,130]. The assessment of an HC involves four aspects: the number of cysts, the content (biliary, serous, proteinaceous, necrotic, hemorrhagic, or mixed), morphology (wall thickness, septa, solid component, enhancement), and clinical background[131,132].

The presence of a solitary or few HC may suggest simple hepatic cysts (SHC), infectious lesions, benign or malignant primary tumors, and metastases1[33].

The SHC is part of the ductal plate malformations[134]. SHC comes from a biliary duct that is separated from the remnant biliary system with further cystic dilatation[135]. It is the most frequent hepatic lesion (~2.5% of the general population), usually asymptomatic[135,136]. The imaging findings are typical. On CT, it is hypo-attenuating (0-20 HU). On MRI, SHC has a low signal on T1w images and the typical strong hyperintensity on T2w images, with a thin, well-defined wall, without contrast enhancement or mural nodules[133]. Rarely, complications such as hemorrhage, infection, rupture, or mass effect of larger cysts must be recognized to avoid misdiagnosis1[29,137].

Infectious lesions rarely appear as a SHC[138]. The colonization by the infectious agent can be from the bloodstream or contiguity (I.e., biliary tree), eventually on altered or necrotic parenchyma[139,140]. Radiological findings partially depend on the etiological factor[138]. Pyogenic abscesses (PA) are the most frequent among the visceral abscesses, and they are often symptomatic (pain and fever are present in up to 75% and 90% of cases)[138]. Escherichia Coli, Klebsiella Pneumoniae, and Streptococci are the most frequent causes by contiguity or hematogenous spread[141-143]. After a pre-suppurative phase, the lesion progresses to a cluster of cystic lesions, which coalesce into a single cyst with irregular walls and septations[132,133]. The content has a variable aspect on CT and MRI; gas bubbles may be present[144-147]. The enhancement of perilesional liver parenchyma is also variable: an eventual inner, hyperenhancing layer of granulomatous tissue may be surrounded by an external edematous hypoenhancing layer[129,130].

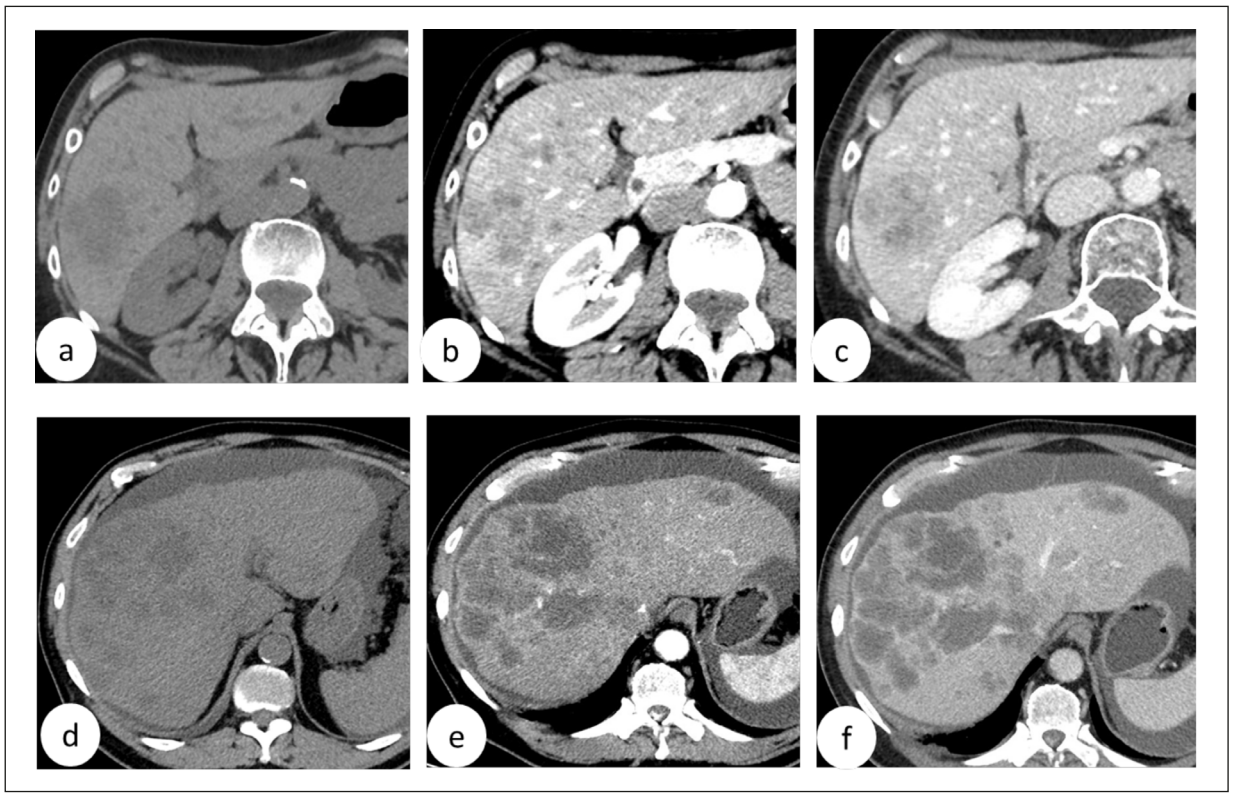


**Figure 4.** Liver metastases: breast (**a-c**), and colorectal cancer (**d-f**) on CT. Basal acquisition (**a,d**). Contrast study: late arterial (**b,e**), and portal venous (**c,f**) phases. Liver metastases from breast adenocarcinoma show heterogeneous hyperenhancement mainly on the periphery with perilesional enhancement (**a-c**). Colorectal liver metastases (**d-f**) appear mostly hypovascular with hypodense, non-enhancing areas giving the appearance of complex cyst.

Amoebic abscesses (Entamoeba Histolitica) are relatively rare in the Western world, but their clinical aspect is similar to PA[144,148]; the clinical data are helpful for the differential diagnosis[149]. Hydatid cysts (Echinococcus Granulosus) are frequent in underdeveloped areas and in people who live in contact with animals (e.g., sheep)[150,151]. Most hydatid infections are asymptomatic, and overlooked, unless complications[150-152]. The categories of Gharbi and the World Health Organization (WHO) classifications are based on the reproductive stage of the parasite matched with the correspondent imaging findings: they range from the simple, thin-wall cyst to intralesional membranes or daughter cysts (all fertile stages), and the inactive cysts (solid or calcified)[153,154].

The presence of solid, enhancing components (complex cysts, i.e., thick wall, septa, nodules) suggests the neoplastic origin of the solitary cyst[130]. Metastases are the most common malignant lesions in the non-cirrhotic liver; less frequently, they may present a cystic aspect[130,155]. The causes may rely on a rapid growth not supported by the vascular supply of the hypervascular metastases (e.g., neuroendocrine tumors, melanomas, or gastrointestinal stromal tumors, GIST) or necrosis after treatment (e.g., GIST)[156-158]. Adenocarcinomas producing mucin (e.g., ovarian or colorectal cancer, Figure 4) may also give cystic liver metastases[157]. The imaging findings are usually non-specific, the differential diagnosis with primary cystic tumors is based on the clinical history of a primary tumor[130,135]. Mucinous cystic tumors (MCT) and intraductal papillary neoplasms of the biliary ducts (IPNB) are rare primary cystic tumors[159]. They have a variable malignant potential (6% for MCT, 40-80% for IPNB), the first can be described as a complex cyst, while the latter has communication with the biliary tree[159]. Imaging findings, such as nodules and wall enhancement, are correlated with malignancy of MCT, but with limited diagnostic yeld[160,161].

The presence of multiple hepatic cysts can be related to congenital abnormalities[133]. Ductal plate malformations can involve intrahepatic or extrahepatic ducts and derive from the insufficient remodeling of the cylindrical ductal plate[134]. The different malformations are related to the stage

of the ductal plate abnormalities from the main to the peripheral ducts[134]. Biliary Hamartomas (BH) are small, interlobular bile ducts not involuted during late embryogenesis, with a prevalence of up to 5.6% in the general population[162,163]. On CT and MRI, usually, multiple BH is scattered through the parenchyma, with the classical "starry sky" sign at MR cholangiography: at MRI, the absence of communication with the intrahepatic bile ducts can be demonstrated. Occasionally, BH can demonstrate a rim enhancement of the surrounding parenchyma in post-contrast studies; small, enhancing mural nodules may represent the polypoid projection[162,164,165]. Caroli disease and syndrome (CD and CS) are rare ductal plate abnormalities[166]. The first is an abnormal development of the large bile ducts during the early remodeling of the ductal plate; the second involves both the large and the peripheral bile ducts during the early and late remodeling of the ductal plate and is associated with congenital hepatic fibrosis[166]. At MRI, CD shows dilated biliary ducts communicating with the biliary system (this can also be demonstrated with HSCA)[166]. The central dot sign in CD is a residual portal and arterial branch within the dilated duct[133,166]. The CS has similar findings associated with parenchymal dysmorphia and portal hypertension of the congenital fibrosis – a different management is required due to the increased risk of CCC[166]. Polycystic liver disease (at least 10 cysts) may be isolated to the liver (autosomal dominant) or also involve the kidney (autosomal dominant or recessive); the symptoms are related to the mass effect[167]. Finally, the peribiliary cysts are abnormal dilation of extramural peribiliary glands[133]. On MRI, ectasic peribiliary glands show the typical "string of pearl" sign; the absent communication with the biliary tree can be demonstrated even with HSCA[133,168].

## An overview of liver metastases: from hypovascular to hypervascular lesions

The term "hypovascular" and "hypervascular" are not standardized in the LI-RADS lexicon[102]. In general, they refer to the relative enhancement of the lesion compared to the liver[155,169].

Liver metastases (LM) have a wide spectrum of imaging findings, depending on the primary tumors, differentiation, histologic behavior (e.g., solid or mucinous), eventual complications, and conditions of the surrounding parenchyma[170]. Many malignancies, mainly from the gastrointestinal tract, preferentially metastasize to the liver, followed by other primary sites[171]. Many factors affect the phenomenon, such as the huge amount of systemic and portal blood flowing to the liver, the sinusoidal fenestration, and the effect of exosomes on the Kuppfer cells in the formation of metastatic niche[172-174]. LMs usually have an arterial supply. Thus they can be classified on the arterial flow[175,176]. Hypovascular LMs have reduced enhancement than the liver and are better depicted on the portal phase; hypervascular LMS enhance more than the liver with venous washout or fade[169,177].

The paradigm of the hypovascular lesion is the LM from adenocarcinomas of the gastrointestinal tract (Figure 4)[170]. The typical architecture consists of a central core with variable aspects: desmoplastic, necrotic, or hemorrhagic[176,178-181]. The peripheral, growing portion of the metastasis is classified into different categories at pathology: desmoplastic, pushing, and infiltrative, while the sinusoidal and portal are rare[176,178,180]. In the desmoplastic pattern, the LM is surrounded by a fibrous band of fibrotic tissue which contributes to the perilesional enhancement due to vascular compression, the opening of arterioportal shunts, and inflammatory infiltrates; it is usually associated with a better prognosis[169,180,182-184]. In some cases, the effects of the LM on the surrounding parenchyma are detected on CT or MRI as perilesional enhancement (which is different from rim APHE)[185]. Currently, a hypothetical correlation between the lesion borders on CT and MRI and the pushing or infiltrative pattern has not been demonstrated[186]. Globally, the variable aspect of the lesion core (i.e., fibrosis, necrosis, hemorrhage), the concentration of the viable tumor at the periphery, and the effects on the surrounding parenchyma are responsible for the targetoid aspect on T2w images, DWI, and on contrast studies[109,170].

Conversely, malignancies such as NET, GIST, melanoma, sarcomas, renal cell carcinomas, thyroid, and breast carcinomas are frequently hypervascular: a known primary malignancy or a chronic liver disease are helpful for the differential diagnosis with HCC[114,187-189]. Common characteristics of these lesions is the *APHE* (rim or nonrim, Figure 4) due to the significant neoangiogenesis[190-197]. The washout or fade is variable across the different hypervascular metastases and sometimes provides useful information about the primary malignancy[177,190,198,199]. Finally, the signal intensity on T1 and T2 images is variable due to several factors (e.g., melanin, necrosis, or hemorrhage); on DWI a restricted diffusion is usually noticed[200-204].

## Hypervascular Liver Lesions: Benign and Malignant Entities

A broad variety of liver lesions are hypervascular (i.e., they present APHE), and their differential diagnosis is sometimes challenging[188].

HH is the most frequent hypervascular lesion after HC (Figure 2)[205]. The structure of HH explains the imaging findings. It is a mesenchymal lesion composed of multiple vascular spaces with hampered blood flow[122]. At MRI, the typical T2 marked hyperintensity derived to the nearly-still blood within the vascular spaces without any restriction on DWI[206]. The contrast enhancement, both on CT and MRI, parallels the blood pool. Thus, the attenuation or the signal is comparable to the vascular compartment better depicted in the respective phase[109,207]. The most common subtype is cavernous hemangioma, where the large vascular spaces are responsible for peripheral nodular enhancement. In larger lesions, the signal can be inhomogeneous and the progressive, centripetal enhancement can be incomplete in late phases[109,208]. The flash-filling hemangioma is rarer (16% of HH); the difference with cavernous HH is in the rapid enhancement, which parallels the blood pool[122]. Other rare, atypical findings are related to the evolution of HH or complications[207]. The centrifugal enhancement of HH can be explained by the peripheral fibrosis of the lesion[122]. The sclerosing and sclerosed HH are the end-stage of the fibrotic evolution of HH, particularly in the cirrhotic liver[209-211]. While calcifications are relatively frequent, other aspects like fluid-fluid levels, and multicystic or pedunculated HH are less frequent[122,207].

Focal Nodular Hyperplasia (FNH) has an incidence of 0.9% and is the second most benign lesion after HH (Figure 1)[212]. Pathologically, FNH is a hyperplastic, regenerative response to an abnormal portal flow[212]. The main features of pathology are the central fibrovascular scar with the arterial supply and the ductular proliferation without the development of the portal tract[213]. The potential of malignant transformation is null[213]. MRI is considered the gold standard for the assessment of FNH[214]. At basal acquisitions, FNH typically has a mild-moderate T2 hyperintensity and is hypointense on T1w images[215]. The overlap with the other lesions on DWI-ADC images limits the diagnostic performance of this sequence[216,217]. In contrast studies, the central scar is visible in 60% (CT) and 80% (MRI) of cases with delayed enhancement. FNH shows the typical APHE with slight hyperintensity on portal venous phase or fade[215,218,219]. The active uptake of HSCA by the normal hepatocytes reflects the 4 different patterns on the hepatobiliary phase: homogeneous and heterogeneous hyperintensity, isointensity, hypointensity with peripheral ring uptake[72,218-220]. Few caveats must be pointed on the hepatobiliary phase. The perilesional HSCA retention from hepatocellular reaction to CCC and metastases must be differentiated from the peripheral ring uptake of FNH; a targetoid aspect with central hyperintensity suggests retention from fibrous tissue (e.g., metastases) rather than the active uptake of FNH[221].

Hepatocellular adenoma (HA) is ten times less frequent than FNH[222]. It is detected mainly in young females and has a correlation with an abnormal exposure or metabolism of sexual hormones, obesity, glucose storage diseases, maturity-onset diabetes and other complex syndromes (Figure 1)[222]. At pathology, HA is a benign, clonal hepatocellular neoplasm with a potential evolution to malignancy of 5%: this requires a different management than FNH[223-225]. The HA are classified in molecular subtypes: inactivation of hepatocyte nuclear factor 1 alpha (HNF1α, 15-40%), inflammatory (18-44%), telangiectatic (previously included among FNH, with the expression of serum amyloid protein, SAA, and C-reactive protein, CRP), activation of β-catenin (with the highest potential of malignant transformation), mixed inflammatory and β-catenin, activation of sonic hedgehog (4%), and unclassified (7-23%)[226]. Typical features of HA are intralesional fat, detectable at chemical-shift MRI, various hyperintensity on T2w images, APHE with fade or washout, and a reduced uptake of HSCA with hypointensity on the hepatobiliary phase[218,219]. Some studies[223,227] aimed to correlate the imaging findings on MRI with the molecular subtypes, e.g., the presence of intralesional fat and moderate APHE in HNF1α, or the atoll sign (i.e., peripheral rim hyperintensity) on T2w with the inflammatory subtype. Though the hypointensity on hepatobiliary phase was considered the most important finding for the differential diagnosis with FNH, its accuracy may have been overestimated due to several factors. The small case series, the misclassification of inflammatory HA within FNH, the absence of molecular data, the active uptake of HSCA by some HA, may lead to misclassification of these lesions in the published data; thus, a more integrated assessment of MRI findings is warranted[214,227-230]. The differential diagnosis may be more complex when

other hypervascular lesions are involved in the differential diagnosis with FNH and HA[231].

An important differential diagnosis of FNH and HA is HCC and its fibrolamellar variant on non-cirrhotic liver (Figure 3)[232]. HCC on non-cirrhotic liver presents similar imaging findings of HCC on cirrhotic liver but more often at a more advanced stage (satellite nodules, neoplastic portal vein thrombi, metastases) due to the lack of surveillance[176,232]. Fibrolamellar HCC is rare, with a peak incidence in the 2nd-3rd decade of life, comparable to FNH and HA. Fibrolamellar HCC typically presents heterogeneous APHE with washout or fade with hypointensity on hepatobiliary phase[232]. Key points for the differential diagnosis are calcifications (rare in FNH and HA), a bigger scar than FNH, the heterogeneous APHE (homogeneous in FNH), and lack of intralesional fat or hemorrhage (more frequent in HA)[232].

CCC is the second malignancy on non-cirrhotic liver after LMs and on cirrhotic liver after HCC; the most common risk factor is the chronic inflammation of the biliary system (Figure 3)[111,233]. CCC is classified as intrahepatic (iCCC, proximal to the 2nd order bile ducts), perihilar (to the confluence of the cystic duct), and distal (to the papilla major)[234]. CCC has three growth patterns: mass-forming, intraductal, periductal infiltrating type[111,235]. At pathology, the vast majority of CCC are mass-forming[234]. They are non-capsulated nodules with peripheral, growing cellular compartment and a central, firm, fibrous component; other non-classical aspects (e.g., mucinous) are more rare[234,236,237]. On CT, iCCC is typically hypo-attenuating, with peripheral, early enhancement corresponding to the neoplastic cellular component (rim APHE) while the central fibrous compartment enhances progressively in the delayed phases[234]. On MRI, a targetoid aspect on T2w and DWI can be detected, with similar findings at the contrast study[111,235,238]. Capsular retraction, parenchymal hypotrophy, satellite nodules and vascular encasement, rarely with tumor thrombi, are the effect of the infiltrative behaviour[111,235,239]. The use of HSCA may be beneficial for the characterization and intra-hepatic staging of iCCC: a mosaic hypointensity or targeted aspect on hepatobiliary phase is more frequent in iCCC (targetoid aspect of LI-RADS M category) than in HCC[109,240].

The differential diagnosis of other rare hypervascular lesions is beyond the aim of this paper and are described elsewhere[111,114,241].

## Chronic Liver Disease: Focus on HCC

HCC is the most frequent malignant tumor in chronic liver disease (CLD)[5]. Several risk factors are responsible of CLD (e.g., viral, metabolic, toxic…); they sustain chronic, inflammatory damage to the liver parenchyma with a wide, progressive spectrum of damage, from steatosis to fibrosis and cirrhosis[242]. Historically, the role of imaging in the assessment of CLD was limited. In fact, the typical morphological changes such as the relative hypertrophy of the left and caudate lobe, areas of parenchymal atrophy or confluent fibrosis, the expansion of the gallbladder fossa and perihilar space, altered signal or density are typical of advanced stages of CLD[85,243-246]. The efforts for the noninvasive assessment of CLD at imaging started with Doppler evaluation of portal hypertension and the hepatic vascularization globally as a consequence of cirrhosis, with ongoing studies on advanced US and MRI techniques[247-252]. Elastography techniques with ultrasound were subsequently introduced to assess parenchyma stiffness, being the management of cirrhosis one of the main applications[253,254]. MR elastography has shown promising results, but its utilization is less diffuse[255]. Other advanced techniques based on artificial intelligence are still in the experimental field[256-260]. The epidemiology of CLD is changing after the introduction of the newer antivirals and with the increase of metabolic diseases: while MRI is considered the gold standard for noninvasive assessment of steatosis, CT and ultrasound are active fields of research[261-266].

The progression of the disease leads to the progressive impairment of liver function with multisystemic consequences and the necessity of transplantation[267-270]. During the progression of CLD, chronic inflammation also leads to hepatocarcinogenesis: the accurate diagnosis of HCC and the tumor burden is fundamental for the eligibility for transplantation or specific treatments[5,267,271,272]. At pathology, hepatocarcinogenesis is a continuous process toward de-differentiation with the development of clonal hepatocellular populations leading to HCC[273,274]. Cirrhotic or regenerative nodules are surrounded by fibrosis and are the result of the remodeling of liver parenchyma: hepatocytes are normal without any clonality[275]. The dysplastic nodules (DN) are classified in low- and high-grade: the first have clone-like populations and unpaired arteries, while the high-grade DN have cellular atypia,

trabeculae or pseudoglands[133,273]. Early HCC is the analogous of the carcinoma in situ of other districts; the difference with the high-grade DN is the stromal invasion, although the growth pattern is not properly infiltrative[276]. The progressed HCC has infiltrative or expansile growth pattern and the ability to metastasize[277].

Several histological changes occur during hepatocarcinogenesis, detectable at imaging[274]. Neoangiogenesis is characterized by unpaired arteries (not matched with the portal triads) and sinusoidal capillarization (basal membranes with loss of fenestrae): both appear in dysplastic nodules and subsequent steps of hepatocarcinogenesis[278]. The venous drainage changes from the hepatic veins (until early HCC) to sinusoids (progressed HCC without fibrous capsule) and portal veins (progressed HCC with fibrous capsule): this contributes to the corona enhancement in progressed HCC and may explain portal vein tumors[109,279,280]. The capsule formation is a fibrovascular structure typical of progressed HCC[277]. The metabolic changes involve the OATP and MRP (multi-drug resistance protein) transporters detected with HSCA, the first being reduced in the high-grade DN and subsequent lesions[281].

Globally, these pathological alterations explain the radiological findings used for the non-invasive diagnosis of HCC (Figure 3)[282]. The proportion of unpaired arteries and reduced portal tracts are responsible of the reduced blood supply of the high-grade DN, and of the APHE of HCC; the mechanisms behind washout and corona enhancement are more complex and non-completely understood[283]. Thus, the first radiological finding of hepatocarcinogenesis is the reduced uptake of HSCA; it is followed by washout in the high-grade DN, APHE in HCC, and the capsule appearance and corona enhancement of progressed HCC[109,283,284]. The actual guidelines in the Western world rely on these criteria: the European Association for the study of the Liver (EASL) considered the wash-in (non-rim APHE) and the washout (nonperipheral), independently in the use of HSCA; the LI-RADS categories (in particular from 3 to 5, with increasing probability of HCC at pathology) are assigned on lesion diameter, non-rim APHE, nonperipheral washout and growth while other CT and MRI findings are considered as ancillary features[5,6,74,109]. For a more detailed review of pathological and imaging findings in HCC, please refer to the study by Choi et al[283,284].

## Beyond Imaging: When to Biopsy?

Liver biopsy is an invasive procedure with reduced, but not negligible, risk of complications, and its use should be relegated to specific cases[285]. The ACR proposed an algorithm for the management of incidental liver lesions on CT[3]. The first discriminant is the lesion diameter (<1 cm, 1-1.5 cm; >1.5 cm); then, the patients are classified in low- or high-risk on the presence of chronic liver diseases or known malignancy. The third step is lesion characterization. In case of hypervascular lesions or in the presence of features suggestive for malignancy (e.g., targetoid aspect, MRI, metabolic imaging (e.g., PET/CT), or biopsy are particularly recommended for larger lesions[3,286,287].

Conversely, in CLD, the high pre-test probability of HCC limits the use of biopsy. In the EASL guidelines, the biopsy is suggested after at least two inconclusive radiological examinations[222]. On the other hand, the indications for liver biopsy in the LI-RADS system are different[288]. Liver biopsy is indicated if the histological or molecular characterization is necessary for treatment or clinical trials, in case of LI-RADS M category or diffuse malignancy, in the presence of extrahepatic malignancy, in selected cases of LI-RADS 3 and 4 categories, or LI-RADS 5 observations in subjects not at risk[6,109,288,289].

## Conclusions

The occurrence of a liver lesion in routine clinical imaging is a frequent event. The differential diagnosis may be challenging for the beginner. The comprehensive, organized, and standardized evaluation of imaging findings, explained by their pathological background, together with clinical data and risk factors, allows, in most cases, the accurate diagnosis of liver lesions.

### Ethics Approval and Informed Consent

This narrative review did not involve any human subject or animal. The ethics approval and informed consent are not applicable.

### Conflict of Interest

AA is a speaker for Siemens Healthineers. The other authors have no conflict of interest to disclose.

### Availability of Data and Materials

Not applicable.

### Acknowledgements
Not applicable.

### ORCID ID
Alessandra Borgheresi: 0000-0002-5544-9468
Andrea Agostini: 0000-0002-0693-8257
Andrea Giovagnoni: 0000-0002-5264-652X

### Authors' Contribution
Literature search, writing – original draft preparation, and manuscript editing: A.B., A.A., L.P., A.Z., S.C-C., M.G., F.D.M., M.C.B., F.B., P.P., F.G., R.F., V.G. Manuscript editing and approval, and supervision: N.G., V.M., A.B., A.G. All authors have read and agreed to the published version of the manuscript. The authors confirm that the article is not under consideration for publication elsewhere. Each author has participated sufficiently to take public responsibility for the manuscript content.

## References

1) Gore RM, Thakrar KH, Wenzke DR, Newmark GM, Mehta UK, Berlin JW. That liver lesion on MDCT in the oncology patient: is it important? Cancer Imaging 2012; 12: 373-384.
2) Lorusso F, Principi M, Pedote P, Pignataro P, Francavilla M, Sardaro A, Scardapane A. Prevalence and clinical significance of incidental extra-intestinal findings in MR enterography: experience of a single University Centre. Radiol Med 2021; 126: 181-188.
3) Gore RM, Pickhardt PJ, Mortele KJ, Fishman EK, Horowitz JM, Fimmel CJ, Talamonti MS, Berland LL, Pandharipande PV. Management of Incidental Liver Lesions on CT: A White Paper of the ACR Incidental Findings Committee. J Am Coll Radiol 2017; 14: 1429-1437.
4) Chernyak V, Tang A, Do RKG, Kamaya A, Kono Y, Santillan CS, Fowler KJ, Bashir MR, Cunha GM, Fetzer DT, Kielar A, Lee JT, Mendiratta-Lalla M, Sirlin CB, Acknowledgements and the LRSC and G of translation integrity listed in the. Liver imaging: it is time to adopt standardized terminology. Eur Radiol 2022; 32: 6291-6301.
5) European Association for the Study of the Liver, Galle PR, Forner A, Llovet JM, Mazzaferro V, Piscaglia F, Raoul JL, Schirmacher P, Vilgrain V. EASL Clinical Practice Guidelines: Management of hepatocellular carcinoma. J Hepatol 2018; 69: 182-236.
6) American College of Radiology Committee on LI-RADS® (Liver). Chapter 8. LIRADS Diagnostic Categories. LI-RADS® v2018. CT/MRI Manual. Published 2018. Accessed December 21, 2022. Available at: https://www.acr.org/-/media/ACR/Files/Clinical-Resources/LIRADS/Chapter-8-LI-RADS-Categories.pdf?la=en&;hash=6008F7A-3B8E2475E4C1DC2C8974A052D.
7) Chernyak V, Fowler KJ, Kamaya A, Kielar AZ, Elsayes KM, Bashir MR, Kono Y, Do RK, Mitchell DG, Singal AG, Tang A, Sirlin CB. Liver Imaging Reporting and Data System (LI-RADS) Version 2018: Imaging of Hepatocellular Carcinoma in At-Risk Patients. Radiology 2018; 289: 816-830.
8) Borghesi A, Sverzellati N, Polverosi R, Balbi M, Baratella E, Busso M, Calandriello L, Cortese G, Farchione A, Iezzi R, Palmucci S, Pulzato I, Rampinelli C, Romei C, Valentini A, Grassi R, Larici AR. Impact of the COVID-19 pandemic on the selection of chest imaging modalities and reporting systems: a survey of Italian radiologists. Radiol Med 2021; 126: 1258-1272.
9) Fowler KJ, Bashir MR, Fetzer DT, Kitao A, Lee JM, Jiang H, Kielar AZ, Ronot M, Kamaya A, Marks RM, Elsayes KM, Tang A, Sirlin CB, Chernyak V. Universal Liver Imaging Lexicon: Imaging Atlas for Research and Clinical Practice. Radiographics 2023; 43: e220066.
10) American College of Radiology Committee on LI-RADS® (Liver). Liver Reporting & Data System (LI-RADS®) v2018. Published 2018. Accessed December 18, 2022. Available at: https://www.acr.org/Clinical-Resources/Reporting-and-Data-Systems/LI-RADS
11) Fowler KJ, Brown JJ, Narra VR. Magnetic resonance imaging of focal liver lesions: Approach to imaging diagnosis. Hepatology 2011; 54: 2227-2237.
12) Rampado O, Depaoli A, Marchisio F, Gatti M, Racine D, Ruggeri V, Ruggirello I, Darvizeh F, Fonio P, Ropolo R. Effects of different levels of CT iterative reconstruction on low-contrast detectability and radiation dose in patients of different sizes: an anthropomorphic phantom study. Radiol Med 2021; 126: 55-62.
13) Chung BM, Park HJ, Park SB, Lee JB, Ahn HS, Kim YS. Differentiation of small arterial enhancing hepatocellular carcinoma from non-tumorous arterioportal shunt with an emphasis on the precontrast CT scan. Abdom Imaging 2015; 40: 2200-2209.
14) Hennedige T, Yang ZJ, Ong CK, Venkatesh SK. Utility of non-contrast-enhanced CT for improved detection of arterial phase hyperenhancement in hepatocellular carcinoma. Abdom Imaging 2014; 39: 1247-1254.
15) Flemming B, Kovacs MD, Hardie A, Picard M, Burchett PF, Collins H, Sheafor DH. Non-contrast and portal venous phase computed tomography in breast cancer hepatic metastases: comparison of tumor measurements and impact on response assessment. Acta Radiologica Open 2021; 10: 2058460121998015.
16) Laghi A, Iannaccone R, Rossi P, Carbone I, Ferrari R, Mangiapane F, Nofroni I, Passariello R. Hepatocellular Carcinoma: Detection with Triple-Phase Multi–Detector Row Helical CT in Patients with Chronic Hepatitis. Radiology 2003; 226: 543-549.
17) Ichikawa T, Kitamura T, Nakajima H, Sou H, Tsukamoto T, Ikenaga S, Araki T. Hypervascular Hepatocellular Carcinoma: Can Double Arterial

Phase Imaging with Multidetector CT Improve Tumor Depiction in the Cirrhotic Liver? Am J Roentgenol 2002; 179: 751-758.

18) Bae KT. Intravenous Contrast Medium Administration and Scan Timing at CT: Considerations and Approaches1. Radiology 2010; 256: 32-61.

19) Kulkarni NM, Fung A, Kambadakone AR, Yeh BM. Computed Tomography Techniques, Protocols, Advancements, and Future Directions in Liver Diseases. Magn Reson Imaging C 2021; 29: 305-320.

20) American College of Radiology Committee on LI-RADS® (Liver). Chapter 12. Technique. LI-RADS® v2018. CT/MRI Manual. Published 2018. Accessed December 21, 2022. Available at: https://www.acr.org/-/media/ACR/Files/Clinical-Resources/LIRADS/Chapter-12-Technique.pdf?la=en&;hash=3B774BD8A6D0A-6ACBD62B2330705FD14

21) Lam A, Fernando D, Sirlin CC, Nayyar M, Goodwin SC, Imagawa DK, Lall C. Value of the portal venous phase in evaluation of treated hepatocellular carcinoma following transcatheter arterial chemoembolisation. Clin Radiol 2017; 72: 994.e9-994.e16.

22) Liu YI, Kamaya A, Jeffrey RB, Shin LK. Multidetector Computed Tomography Triphasic Evaluation of the Liver Before Transplantation. J Comput Assist Tomo 2012; 36: 213-219.

23) Liu YI, Shin LK, Jeffrey RB, Kamaya A. Quantitatively Defining Washout in Hepatocellular Carcinoma. Am J Roentgenol 2013; 200: 84-89.

24) Zanca F, Brat HG, Pujadas P, Racine D, Dufour B, Fournier D, Rizk B. Prospective multicenter study on personalized and optimized MDCT contrast protocols: results on liver enhancement. Eur Radiol 2021; 31: 8236-8245.

25) Kondo H, Kanematsu M, Goshima S, Watanabe H, Kawada H, Moriyama N, Bae KT. Body size indices to determine iodine mass with contrast-enhanced multi-detector computed tomography of the upper abdomen: does body surface area outperform total body weight or lean body weight? Eur Radiol 2013; 23: 1855-1861.

26) Masuda T, Nakaura T, Funama Y, Higaki T, Kiguchi M, Imada N, Sato T, Awai K. Aortic and Hepatic Contrast Enhancement During Hepatic-Arterial and Portal Venous Phase Computed Tomography Scanning. J Comput Assist Tomo 2017; 41: 309-314.

27) Schima W, Hammerstingl R, Catalano C, Marti-Bonmati L, Rummeny EJ, Montero FT, Dirisamer A, Westermayer B, Bellomi M, Brisbois D, Chevallier P, Dobritz M, Drouillard J, Fraioli F, Martinez MJ, Morassut S, Vogl TJ. Quadruple-Phase MDCT of the Liver in Patients with Suspected Hepatocellular Carcinoma: Effect of Contrast Material Flow Rate. Am J Roentgenol 2006; 186: 1571-1579.

28) Saade C, Karout L, Asmar KE, Naffaa L, Merhi FE, Salman R, Abi-Ghanem AS. Impact of various iodine concentrations of iohexol and iodixanol contrast media on image reconstruction techniques in a vascular-specific contrast media phantom: quantitative and qualitative image quality assessment. Radiol Med 2021; 126: 221-230.

29) Amis ES, Butler PF, Applegate KE, Birnbaum SB, Brateman LF, Hevezi JM, Mettler FA, Morin RL, Pentecost MJ, Smith GG, Strauss KJ, Zeman RK, Radiology AC of. American College of Radiology White Paper on Radiation Dose in Medicine. J Am Coll Radiol 2007; 4: 272-284.

30) Compagnone G, Padovani R, D'Ercole L, Orlacchio A, Bernardi G, D'Avanzo MA, Grande S, Palma A, Campanella F, Rosi A. Provision of Italian diagnostic reference levels for diagnostic and interventional radiology. Radiol Med 2021; 126: 99-105.

31) Takahashi H, Okada M, Hyodo T, Hidaka S, Kagawa Y, Matsuki M, Tsurusaki M, Murakami T. Can low-dose CT with iterative reconstruction reduce both the radiation dose and the amount of iodine contrast medium in a dynamic CT study of the liver? Eur J Radiol 2014; 83: 684-691.

32) Noda Y, Kanematsu M, Goshima S, Kondo H, Watanabe H, Kawada H, Kawai N, Tanahashi Y, Miyoshi TRT, Bae KT. Reducing iodine load in hepatic CT for patients with chronic liver disease with a combination of low-tube-voltage and adaptive statistical iterative reconstruction. Eur J Radiol 2015; 84: 11-18.

33) Agostini A, Borgheresi A, Granata V, Bruno F, Palumbo P, Muzio FD, Bicci E, Grazzini G, Grassi F, Fusco R, Barile A, Miele V, Giovagnoni A. Technological advances in body CT: a primer for beginners. Eur Rev Med Pharmacol Sci 2022; 26: 7918-7937.

34) Fusco R, Setola SV, Raiano N, Granata V, Cerciello V, Pecori B, Petrillo A. Analysis of a monocentric computed tomography dosimetric database using a radiation dose index monitoring software: dose levels and alerts before and after the implementation of the adaptive statistical iterative reconstruction on CT images. Radiol Med 2022; 127: 733-742.

35) Hur S, Lee JM, Kim SJ, Park JH, Han JK, Choi BI. 80-kVp CT Using Iterative Reconstruction in Image Space Algorithm for the Detection of Hypervascular Hepatocellular Carcinoma: Phantom and Initial Clinical Experience. Korean J Radiol 2011; 13: 152-164.

36) Geyer LL, Schoepf UJ, Meinel FG, Jr JWN, Bastarrika G, Leipsic JA, Paul NS, Rengo M, Laghi A, Cecco CND. State of the Art: Iterative CT Reconstruction Techniques. Radiology 2015; 276: 339-357.

37) Agostini A, Borgheresi A, Carotti M, Ottaviani L, Badaloni M, Floridi C, Giovagnoni A. Third-generation iterative reconstruction on a dual-source, high-pitch, low-dose chest CT protocol with tin filter for spectral shaping at 100 kV: a study on a small series of COVID-19 patients. Radiol Med 2021; 126: 388-398.

38) Mileto A, Guimaraes LS, McCollough CH, Fletcher JG, Yu L. State of the Art in Abdominal CT: The Limits of Iterative Reconstruction Algorithms. Radiology 2019; 293: 191422.

39) Sun J, Li H, Gao J, Li J, Li M, Zhou Z, Peng Y. Performance evaluation of a deep learning image reconstruction (DLIR) algorithm in "double low" chest CTA in children: a feasibility study. Radiol Med 2021; 126: 1181-1188.

40) Nakamura Y, Higaki T, Tatsugami F, Zhou J, Yu Z, Akino N, Ito Y, Iida M, Awai K. Deep Learning–based CT Image Reconstruction: Initial Evaluation Targeting Hypovascular Hepatic Metastases. Radiology Artif Intell 2019; 1: e180011.

41) Agostini A, Borgheresi A, Mari A, Floridi C, Bruno F, Carotti M, Schicchi N, Barile A, Maggi S, Giovagnoni A. Dual-energy CT: theoretical principles and clinical applications. Radiol Med 2019; 124: 1281-1295.

42) Hanson GJ, Michalak GJ, Childs R, McCollough B, Kurup AN, Hough DM, Frye JM, Fidler JL, Venkatesh SK, Leng S, Yu L, Halaweish AF, Harmsen WS, McCollough CH, Fletcher JG. Low kV versus dual-energy virtual monoenergetic CT imaging for proven liver lesions: what are the advantages and trade-offs in conspicuity and image quality? A pilot study. Abdom Radiol 2018; 43: 1404-1412.

43) Ascenti G, Sofia C, Mazziotti S, Silipigni S, D'Angelo T, Pergolizzi S, Scribano E. Dual-energy CT with iodine quantification in distinguishing between bland and neoplastic portal vein thrombosis in patients with hepatocellular carcinoma. Clin Radiol 2016; 71: 938.e1-938.e9.

44) Donato H, França M, Candelária I, Caseiro-Alves F. Liver MRI: From basic protocol to advanced techniques. Eur J Radiol 2017; 93: 30-39.

45) Agostini A, Kircher MF, Do RKG, Borgheresi A, Monti S, Giovagnoni A, Mannelli L. Magnetic Resonanance Imaging of the Liver (Including Biliary Contrast Agents)—Part 2: Protocols for Liver Magnetic Resonanance Imaging and Characterization of Common Focal Liver Lesions. Semin Roentgenol 2016; 51: 317-333.

46) Guglielmo FF, Mitchell DG, Roth CG, Deshmukh S. Hepatic MR Imaging Techniques, Optimization, and Artifacts. Magn Reson Imaging C 2014; 22: 263-282.

47) Augui J, Vignaux O, Argaud C, Coste J, Gouya H, Legmann P. Liver: T2-weighted MR Imaging with Breath-hold Fast-Recovery Optimized Fast Spin-Echo Compared with Breath-hold Half-Fourier and Non–Breath-hold Respiratory-triggered Fast Spin-Echo Pulse Sequences. Radiology 2002; 223: 853-859.

48) Constable RT, Anderson AW, Zhong J, Gore JC. Factors influencing contrast in fast spin-echo MR imaging. Magn Reson Imaging 1992; 10: 497-511.

49) McFarland EG, Mayo-Smith WW, Saini S, Hahn PF, Goldberg MA, Lee MJ. Hepatic hemangiomas and malignant tumors: improved differentiation with heavily T2-weighted conventional spin-echo MR imaging. Radiology 1994; 193: 43-47.

50) Ito K, Mitchell DG, Outwater EK, Szklaruk J, Sadek AG. Hepatic lesions: discrimination of non-solid, benign lesions from solid, malignant lesions with heavily T2-weighted fast spin-echo MR imaging. Radiology 1997; 204: 729-737.

51) Markl M, Leupold J. Gradient echo imaging. J Magn Reson Imaging 2012; 35: 1274-1289.

52) Bley TA, Wieben O, François CJ, Brittain JH, Reeder SB. Fat and water magnetic resonance imaging. J Magn Reson Imaging 2010; 31: 4-18.

53) Shannon BA, Ahlawat S, Morris CD, Levin AS, Fayad LM. Do contrast-enhanced and advanced MRI sequences improve diagnostic accuracy for indeterminate lipomatous tumors? Radiol Med 2022; 127: 90-99.

54) Ream JM, Rosenkrantz AB. Advances in T1-Weighted and T2-Weighted Imaging in the Abdomen and Pelvis. Radiol Clin N Am 2015; 53: 583-598.

55) Bihan DL. Apparent Diffusion Coefficient and Beyond: What Diffusion MR Imaging Can Tell Us about Tissue Structure. Radiology 2013; 268: 318-322.

56) Liheng M, Guofan X, Balzano RF, Yuying L, Weifeng H, Ning Y, Yayun J, Mouyuan L, Guglielmi G. The value of DTI: achieving high diagnostic performance for brain metastasis. Radiol Med 2021; 126: 291-298.

57) Iima M, Bihan DL. Clinical Intravoxel Incoherent Motion and Diffusion MR Imaging: Past, Present, and Future. Radiology 2015; 278: 13-32.

58) Galea N, Cantisani V, Taouli B. Liver lesion detection and characterization: Role of diffusion-weighted imaging. J Magn Reson Imaging 2013; 37: 1260-1276.

59) Wu LM, Hu J, Gu HY, Hua J, Xu JR. Can diffusion-weighted magnetic resonance imaging (DW-MRI) alone be used as a reliable sequence for the preoperative detection and characterisation of hepatic metastases? A meta-analysis. Eur J Cancer 2013; 49: 572-584.

60) Xiong H, Zeng YL. Standard-b-Value Versus Low-b-Value Diffusion-Weighted Imaging in Hepatic Lesion Discrimination. J Comput Assist Tomo 2016; 40: 498-504.

61) Nalaini F, Shahbazi F, Mousavinezhad SM, Ansari A, Salehi M. Diagnostic accuracy of apparent diffusion coefficient (ADC) value in differentiating malignant from benign solid liver lesions: a systematic review and meta-analysis. Br J Radiology 2021; 94: 20210059.

62) Taouli B, Koh DM. Diffusion-weighted MR Imaging of the Liver1. Radiology 2010; 254: 47-66.

63) Lewis S, Dyvorne H, Cui Y, Taouli B. Diffusion-Weighted Imaging of the Liver Techniques and Applications. Magn Reson Imaging C 2014; 22: 373-395.

64) Lee VS, Lavelle MT, Rofsky NM, Laub G, Thomasson DM, Krinsky GA, Weinreb JC. Hepatic MR Imaging with a Dynamic Contrast-enhanced Isotropic Volumetric Interpolated Breath-hold Examination: Feasibility, Reproducibility, and Technical Quality. Radiology 2000; 215: 365-372.

65) Zerunian M, Pucciarelli F, Caruso D, Polici M, Masci B, Guido G, Santis DD, Polverari D, Principessa D, Benvenga A, Iannicelli E, Laghi A. Artificial intelligence based image quality enhancement in liver MRI: a quantitative and qualitative evaluation. Radiol Med 2022; 127: 1098-1105.

66) Xiao YD, Paudel R, Liu J, Ma C, Zhang ZS, Zhou SK. MRI contrast agents: Classification and application (Review). Int J Mol Med 2016; 38: 1319-1326.

67) Agostini A, Kircher MF, Do R, Borgheresi A, Monti S, Giovagnoni A, Mannelli L. Magnetic Resonance Imaging of the Liver (Including Biliary Contrast Agents) Part 1: Technical Considerations and Contrast Materials. Semin Roentgenol 2016; 51: 308-316.

68) Vilgrain V, Beers BEV, Pastor CM. Insights into the diagnosis of hepatocellular carcinomas with hepatobiliary MRI. J Hepatol 2016; 64: 708-716.

69) Gupta RT, Brady CM, Lotz J, Boll DT, Merkle EM. Dynamic MR Imaging of the Biliary System Using Hepatocyte-Specific Contrast Agents. Am J Roentgenol 2010; 195: 405-413.

70) Granata V, Fusco R, Setola SV, Avallone A, Palaia R, Grassi R, Izzo F, Petrillo A. Radiological assessment of secondary biliary tree lesions: an update. J Int Med Res 2020; 48: 0300060519850398.

71) Zech CJ, Grazioli L, Jonas E, Ekman M, Niebecker R, Gschwend S, Breuer J, Jönsson L, Kienbaum S. Health-economic evaluation of three imaging strategies in patients with suspected colorectal liver metastases: Gd-EOB-DTPA-enhanced MRI vs. extracellular contrast media-enhanced MRI and 3-phase MDCT in Germany, Italy and Sweden. Eur Radiol 2009; 19: 753-763.

72) Zech CJ, Grazioli L, Breuer J, Reiser MF, Schoenberg SO. Diagnostic Performance and Description of Morphological Features of Focal Nodular Hyperplasia in Gd-EOB-DTPA-Enhanced Liver Magnetic Resonance Imaging: Results of a Multicenter Trial. Invest Radiol 2008; 43: 504-511.

73) Zech CJ, Korpraphong P, Huppertz A, Denecke T, Kim M -J., Tanomkiat W, Jonas E, Ba-Ssalamah A, group on behalf of the V study. Randomized multicentre trial of gadoxetic acid-enhanced MRI versus conventional MRI or CT in the staging of colorectal cancer liver metastases. Brit J Surg 2014; 101: 613-621.

74) Gao W, Wang W, Song D, Yang C, Zhu K, Zeng M, Rao S xiang, Wang M. A predictive model integrating deep and radiomics features based on gadobenate dimeglumine-enhanced MRI for postoperative early recurrence of hepatocellular carcinoma. Radiol Med 2022; 127: 259-271.

75) American College of Radiology Committee on LI-RADS® (Liver). Chapter 13. Hepatobiliary Agents. LI-RADS® v2018. CT/MRI Manual. Published 2018. Accessed December 21, 2022. Available at: https://www.acr.org/-/media/ACR/Files/Clinical-Resources/LIRADS/Chapter-13-HBA.pdf?la=en&;hash=7272207E6977F71F-8D4604A27137F2CD.

76) Jang HJ, Lim HK, Lee WJ, Lee SJ, Yun JY, Choi D. Small Hypoattenuating Lesions in the Liver on Single-phase Helical CT in Preoperative Patients with Gastric and Colorectal Cancer: Prevalence, Significance, and Differentiating Features. J Comput Assist Tomo 2002; 26: 718-724.

77) Karhunen PJ. Benign hepatic tumours and tumour like conditions in men. J Clin Pathol 1986; 39: 183-188.

78) Kaltenbach TEM, Engler P, Kratzer W, Oeztuerk S, Seufferlein T, Haenle MM, Graeter T. Prevalence of benign focal liver lesions: ultrasound investigation of 45,319 hospital patients. Abdom Radiol 2016; 41: 25-32.

79) OSHIBUCHI M, NISHI F, SATO M, OHTAKE H, OKUDA K. Frequency of abnormalities detected by abdominal ultrasound among Japanese adults. J Gastroen Hepatol 1991; 6: 165-168.

80) Schwartz LH, Gandras EJ, Colangelo SM, Ercolani MC, Panicek DM. Prevalence and Importance of Small Hepatic Lesions Found at CT in Patients with Cancer. Radiology Published online 1999.

81) Patterson SA, Khalil HI, Panicek DM. MRI Evaluation of Small Hepatic Lesions in Women with Breast Cancer. Am J Roentgenol 2006; 187: 307-312.

82) Krakora GA, Coakley FV, Williams G, Yeh BM, Breiman RS, Qayyum A. Small Hypoattenuating Hepatic Lesions at Contrast-enhanced CT: Prognostic Importance in Patients with Breast Cancer. Radiology 2004; 233: 667-673.

83) Khalil HI, Patterson SA, Panicek DM. Hepatic Lesions Deemed Too Small to Characterize at CT: Prevalence and Importance in Women with Breast Cancer. Radiology 2005; 235: 872-878.

84) Ono Y, Ozawa M, Suzuki K, Okazaki H, Tamura Y, Suzuki T, Suzuki K, Ogawa A, Sugihara S. Autopsy findings of patients with urological neoplasms. Int J Clin Oncol 2002; 7: 0301-0305.

85) Dodd GD, Baron RL, Oliver JH, Federle MP. Spectrum of imaging findings of the liver in end-stage cirrhosis: part I, gross morphology and diffuse abnormalities. Am J Roentgenol 1999; 173: 1031-1036.

86) Dodd GD, Baron RL, Oliver JH, Federle MP. Spectrum of imaging findings of the liver in end-stage cirrhosis: Part II, focal abnormalities. Am J Roentgenol 1999; 173: 1185-1192.

87) Caroli-Bottino A, Nascimento CM, Basto S, Ribeiro J, Silveira V, Carvalho AMS, Castro PN, Villela-Nogueiro CA, Pannain VL. Hepatocellular Carcinoma: Incidental Finding in Cirrhotic Explanted Livers. Transplant P 2005; 37: 2791-2792.

88) Seymour K, Charnley RM. Evidence that metastasis is less common in cirrhotic than normal liver: a systematic review of post-mortem case–control studies. Brit J Surg 1999; 86: 1237-1242.

89) Flusberg M, Ganeles J, Ekinci T, Goldberg-Stein S, Paroder V, Kobi M, Chernyak V. Impact of a Structured Report Template on the Quality of CT and MRI Reports for Hepatocellular Carcinoma Diagnosis. J Am Coll Radiol 2017; 14: 1206-1211.

90) Granata V, Faggioni L, Grassi R, Fusco R, Reginelli A, Rega D, Maggialetti N, Buccicardi D, Frittoli B, Rengo M, Bortolotto C, Prost R, Lacasella GV, Montella M, Ciaghi E, Bellifemine F, Muzio FD, Grazzini G, Filippo MD, Cappabianca S, Laghi A, Grassi R, Brunese L, Neri E, Miele V, Coppola F. Structured reporting of computed tomography in the staging of colon cancer: a Delphi consensus proposal. Radiol Med 2022; 127: 21-29.

91) Corwin MT, Lee AY, Fananapazir G, Loehfelm TW, Sarkar S, Sirlin CB. Nonstandardized Terminology to Describe Focal Liver Lesions in Patients at Risk for Hepatocellular Carcinoma: Implications Regarding Clinical Communication. Am J Roentgenol 2018; 210: 85-90.

92) Agarwal M, Pol CB van der, Patlas MN, Udare A, Chung AD, Rubino J. Optimizing the radiologist work environment: Actionable tips to improve workplace satisfaction, efficiency, and minimize burnout. Radiol Med 2021; 126: 1255-1257.

93) Salvatore C, Roberta F, Angela de L, Cesare P, Alfredo C, Giuliano G, Giulio L, Giuliana G, Maria RG, Paola BM, Fabrizio U, Roberta G, Beatrice F, Vittorio M. Clinical and laboratory data, radiological structured report findings and quantitative evaluation of lung involvement on baseline chest CT in COVID-19 patients to predict prognosis. Radiol Med 2021; 126: 29-39.

94) Freeman RB, Mithoefer A, Ruthazer R, Nguyen K, Schore A, Harper A, Edwards E. Optimizing staging for hepatocellular carcinoma before liver transplantation: A retrospective analysis of the UNOS/OPTN database. Liver Transplant 2006; 12: 1504-1511.

95) Méndez-Sánchez N, Ridruejo E, Mattos AA de, Chávez-Tapia NC, Zapata R, Paraná R, Mastai R, Strauss E, Guevara-Casallas LG, Daruich J, Gadano A, Parise ER, Uribe M, Aguilar-Olivos NE, Dagher L, Ferraz-Neto BH, Valdés-Sánchez M, Sánchez-Avila JF. Latin American Association for the Study of the Liver (LAASL) Clinical Practice Guidelines: Management of Hepatocellular Carcinoma. Ann Hepatol 2014; 13: S4-S40.

96) Bolondi L, Gaiani S, Celli N, Golfieri R, Grigioni WF, Leoni S, Venturi AM, Piscaglia F. Characterization of small nodules in cirrhosis by assessment of vascularity: The problem of hypovascular hepatocellular carcinoma. Hepatology 2005; 42: 27-34.

97) Barabino M, Gurgitano M, Fochesato C, Angileri SA, Franceschelli G, Santambrogio R, Mariani NM, Opocher E, Carrafiello G. LI-RADS to categorize liver nodules in patients at risk of HCC: tool or a gadget in daily practice? Radiol Med 2021; 126: 5-13.

98) Pol CB van der, Lim CS, Sirlin CB, McGrath TA, Salameh JP, Bashir MR, Tang A, Singal AG, Costa AF, Fowler K, McInnes MDF. Accuracy of the Liver Imaging Reporting and Data System in Computed Tomography and Magnetic Resonance Image Analysis of Hepatocellular Carcinoma or Overall Malignancy—A Systematic Review. Gastroenterology 2019; 156: 976-986.

99) Li L, Hu Y, Han J, Li Q, Peng C, Zhou J. Clinical Application of Liver Imaging Reporting and Data System for Characterizing Liver Neoplasms: A Meta-Analysis. Diagnostics 2021; 11: 323.

100) Kierans AS, Song C, Gavlin A, Roudenko A, Lu L, Askin G, Hecht EM. Diagnostic Performance of LI-RADS Version 2018, LI-RADS Version 2017, and OPTN Criteria for Hepatocellular Carcinoma. Am J Roentgenol 2020; 215: 1085-1092.

101) Negroni D, Cassarà A, Trisoglio A, Soligo E, Berardo S, Carriero A, Stecco A. Learning curves in radiological reporting of whole-body MRI in plasma cell disease: a retrospective study. Radiol Med 2021; 126: 1451-1459.

102) American College of Radiology Committee on LI-RADS® (Liver). LI-RADS Lexicon (terms and definitions).

103) American College of Radiology Committee on LI-RADS® (Liver). Chapter 2. LI-RADS® Populations: Surveillance, Diagnosis, Staging, Treatment Response. LI-RADS® v2018. CT/MRI Manual. Published 2018. Accessed December 21, 2022. Available at: https://www.acr.org/-/media/ACR/Files/Clinical-Resources/LIRADS/Chapter-2--LI-RADS-screening-surveillance-diagnosis-staging.pdf?la=en&;hash=5AE5448C1452971CC6E-7130C4B54C037.

104) Renzulli M, Brandi N, Argalia G, Brocchi S, Farolfi A, Fanti S, Golfieri R. Morphological, dynamic and functional characteristics of liver pseudolesions and benign lesions. Radiol Med 2022; 127: 129-144.

105) American College of Radiology Committee on LI-RADS® (Liver). Chapter 7 The LIRADS observation. LI-RADS® v2018. CT/MRI Manual. Published 2018. Accessed December 21, 2022. Available at: https://www.acr.org/-/media/ACR/Files/Clinical-Resources/LIRADS/Chapter-8-LI-RADS-Categories.pdf?la=en&;hash=6008F7A-3B8E2475E4C1DC2C8974A052D.

106) Damadian R. Tumor Detection by Nuclear Magnetic Resonance. Science 1971; 171: 1151-1153.

107) Cameron IL, Ord VA, Fullerton GD. Characterization of proton NMR relaxation times in normal and pathological tissues by correlation with other tissue parameters. Magn Reson Imaging 1984; 2: 97-106.

108) Bottomley PA, Hardy CJ, Argersinger RE, Allen-Moore G. A review of 1H nuclear magnetic resonance relaxation in pathology: Are T1 and T2 diagnostic? Med Phys 1987; 14: 1-37.

109) American College of Radiology Committee on LI-RADS® (Liver). Chapter 16. Imaging features. LI-RADS® v2018. CT/MRI Manual. Published 2018. Accessed December 21, 2022. Available at: https://www.acr.org/-/media/ACR/Files/Clinical-Resources/LIRADS/Chapter-16-Imaging-features.pdf.

110) Hussain HK, Syed I, Nghiem HV, Johnson TD, Carlos RC, Weadock WJ, Francis IR. T2-weighted MR Imaging in the Assessment of Cirrhotic Liver. Radiology 2004; 230: 637-644.

111) Lee DH, Lee JM. Primary malignant tumours in the non-cirrhotic liver. Eur J Radiol 2017; 95: 349-361.

112) Kelekis NL, Semelka RC, Worawattanakul S, Lange EE de, Ascher SM, Ahn IO, Reinhold C, Remer EM, Brown JJ, Bis KG, Woosley JT, Mitchell DG. Hepatocellular carcinoma in North America: a multiinstitutional study of appearance on T1-weighted, T2-weighted, and serial gadolinium-enhanced gradient-echo images. Am J Roentgenol 1998; 170: 1005-1013.

113) Ahn SJ, Kim M, Hong H, Kim KA, Song H. Distinguishing hemangiomas from malignant solid hepatic lesions: A comparison of heavily T2-weighted images obtained before and after administration of gadoxetic acid. J Magn Reson Imaging 2011; 34: 310-317.

114) Silva AC, Evans JM, McCullough AE, Jatoi MA, Vargas HE, Hara AK. MR Imaging of Hypervascular Liver Masses: A Review of Current Techniques1. Radiographics 2009; 29: 385-402.

115) Moigne FL, Durieux M, Bancel B, Boublay N, Boussel L, Ducerf C, Berthezène Y, Rode A. Impact of diffusion-weighted MR imaging on the characterization of small hepatocellular carcinoma in the cirrhotic liver. Magn Reson Imaging 2012; 30: 656-665.

116) Chung JJ, Kim MJ, Kim JH, Lee JT, Yoo HS. Fat Sparing of Surrounding Liver From Metastasis in Patients with Fatty Liver: MR Imaging with Histopathologic Correlation. Am J Roentgenol 2003; 180: 1347-1350.

117) Meloni A, Pistoia L, Restaino G, Missere M, Positano V, Spasiano A, Casini T, Cossu A, Cuccia L, Massa A, Massei F, Cademartiri F. Quantitative T2* MRI for bone marrow iron overload: normal reference values and assessment in thalassemia major patients. Radiol Med 2022; 127: 1199-1208.

118) Shi GZ, Chen H, Zeng WK, Gao M, Wang MZ, Zhang HT, Shen J. R2* value derived from multiecho Dixon technique can aid discrimination between benign and malignant focal liver lesions. World J Gastroentero 2021; 27: 1182-1193.

119) Song W, Chen Q, Guo D, Jiang C. Preoperative estimation of the survival of patients with unresectable hepatocellular carcinoma achieving complete response after conventional transcatheter arterial chemoembolization: assessments of clinical and LI-RADS MR features. Radiol Med 2022; 127: 939-949.

120) Kloeckner R, Santos DP dos, Kreitner KF, Leicher-Düber A, Weinmann A, Mittler J, Düber C. Quantitative assessment of washout in hepatocellular carcinoma using MRI. Bmc Cancer 2016; 16: 758.

121) American College of Radiology Committee on LI-RADS® (Liver). Chapter 15. Benign entities. LI-RADS® v2018. CT/MRI Manual. Published 2018. Accessed December 21, 2022. Available at: https://www.acr.org/-/media/ACR/Files/Clinical-Resources/LIRADS/Chapter-15-Benign-entities.pdf?la=en&;hash=32513D406D328EAE3A9C9E9E15721DC1.

122) Vilgrain V, Boulos L, Vullierme MP, Denys A, Terris B, Menu Y. Imaging of Atypical Hemangiomas of the Liver with Pathologic Correlation. Radiographics 2000; 20: 379-397.

123) Oto A, Kulkarni K, Nishikawa R, Baron RL. Contrast Enhancement of Hepatic Hemangiomas on Multiphase MDCT: Can We Diagnose Hepatic Hemangiomas by Comparing Enhancement With Blood Pool? Am J Roentgenol 2010; 195: 381-386.

124) Sun HY, Lee JM, Shin CI, Lee DH, Moon SK, Kim KW, Han JK, Choi BI. Gadoxetic Acid-Enhanced Magnetic Resonance Imaging for Differentiating Small Hepatocellular Carcinomas (≤2 cm in Diameter) From Arterial Enhancing Pseudolesions. Invest Radiol 2010; 45: 96-103.

125) Ahn SS, Kim MJ, Lim JS, Hong HS, Chung YE, Choi JY. Added Value of Gadoxetic Acid–enhanced Hepatobiliary Phase MR Imaging in the Diagnosis of Hepatocellular Carcinoma. Radiology 2010; 255: 459-466.

126) Haradome H, Unno T, Morisaka H, Toda Y, Kwee TC, Kondo H, Sano K, Ichikawa T, Kondo F, Sugitani M, Takayama T. Gadoxetic acid disodium-enhanced MR imaging of cholangiolocellular carcinoma of the liver: imaging characteristics and histopathological correlations. Eur Radiol 2017; 27: 4461-4471.

127) Zeng D, Xu M, Liang JY, Cheng MQ, Huang H, Pan JM, Huang Y, Tong WJ, Xie XY, Lu MD, Kuang M, Chen LD, Hu HT, Wang W. Using new criteria to improve the differentiation between HCC and non-HCC malignancies: clinical practice and discussion in CEUS LI-RADS 2017. Radiol Med 2022; 127: 1-10.

128) Min JH, Kim YK, Choi SY, Jeong WK, Lee WJ, Ha SY, Ahn S, Ahn HS. Differentiation between cholangiocarcinoma and hepatocellular carcinoma with target sign on diffusion-weighted imaging and hepatobiliary phase gadoxetic acid-enhanced MR imaging: Classification tree analysis applying capsule and septum. Eur J Radiol 2017; 92: 1-10.

129) Borhani AA, Wiant A, Heller MT. Cystic Hepatic Lesions: A Review and an Algorithmic Approach. Am J Roentgenol 2014; 203: 1192-1204.

130) Qian LJ, Zhu J, Zhuang ZG, Xia Q, Liu Q, Xu JR. Spectrum of Multilocular Cystic Hepatic Lesions: CT and MR Imaging Findings with Pathologic Correlation. Radiographics 2013; 33: 1419-1433.

131) Singh Y, Winick AB, Tabbara SO. Multiloculated cystic liver lesions: radiologic-pathologic differential diagnosis. Radiographics 1997; 17: 219-224.

132) Mortelé KJ, Ros PR. Cystic Focal Liver Lesions in the Adult: Differential CT and MR Imaging Features1. Radiographics 2001; 21: 895-910.

133) Chenin M, Paisant A, Lebigot J, Bazeries P, Debbi K, Ronot M, Laurent V, Aubé C. Cystic liver lesions: a pictorial review. Insights Imaging 2022; 13: 116.

134) Desmet VJ. Pathogenesis of Ductal Plate Abnormalities. Mayo Clin Proc 1998; 73: 80-89.

135) Mavilia MG, Pakala T, Molina M, Wu GY. Differentiating Cystic Liver Lesions: A Review of Imaging Modalities, Diagnosis and Management. J Clin Transl Hepatology 2018; 6: 208-216.

136) Gaines PA, Sampson MA. The prevalence and characterization of simple hepatic cysts by ultrasound examination. Br J Radiology 1989; 62: 335-337.

137) Kohno S, Arizono S, Isoda H, Yoshizawa A, Togashi K. Imaging findings of hemorrhagic hepatic cysts with enhancing mural nodules. Abdom Radiol 2019; 44: 1205-1212.

138) Bächler P, Baladron MJ, Menias C, Beddings I, Loch R, Zalaquett E, Vargas M, Connolly S, Bhalla S, Huete Á. Multimodality Imaging of Liver Infections: Differential Diagnosis and Potential Pitfalls. Radiographics 2016; 36: 1001-1023.

139) Lardière-Deguelte S, Ragot E, Amroun K, Piardi T, Dokmak S, Bruno O, Appere F, Sibert A, Hoeffel C, Sommacale D, Kianmanesh R. Hepatic abscess: Diagnosis and management. J Visc Surg 2015; 152: 231-243.

140) Iacobellis F, Serafino MD, Brillantino A, Mottola A, Giudice SD, Stavolo C, Festa P, Patlas MN, Scaglione M, Romano L. Role of MRI in early follow-up of patients with solid organ injuries: How and why we do it? Radiol Med 2021; 126: 1328-1334.

141) Altemeier WA, Culbertson WR, Fullen WD, Shook CD. Intra-abdominal abscesses. Am J Surg 1973; 125: 70-79.

142) Rahimian J, Wilson T, Oram V, Holzman RS. Pyogenic Liver Abscess: Recent Trends in Etiology and Mortality. Clin Infect Dis 2004; 39: 1654-1659.

143) Brizi MG, Perillo F, Cannone F, Tuzza L, Manfredi R. The role of imaging in acute pancreatitis. Radiol Med 2021; 126: 1017-1029.

144) Mortelé KJ, Segatto E, Ros PR. The Infected Liver: Radiologic-Pathologic Correlation. Radiographics 2004; 24: 937-955.

145) Joshi G, Crawford KA, Hanna TN, Herr KD, Dahiya N, Menias CO. US of Right Upper Quadrant Pain in the Emergency Department: Diagnosing beyond Gallbladder and Biliary Disease. Radiographics 2018; 38: 766-793.

146) Alsaif HS, Venkatesh SK, Chan DSG, Archuleta S. CT Appearance of Pyogenic Liver Abscesses Caused by Klebsiella pneumoniae. Radiology 2011; 260: 129-138.

147) Filippo MD, Puglisi S, D'Amuri F, Gentili F, Paladini I, Carrafiello G, Maestroni U, Rio PD, Ziglioli F, Pagnini F. CT-guided percutaneous drainage of abdominopelvic collections: a pictorial essay. Radiol Med 2021; 126: 1561-1570.

148) Congly SE, Shaheen AAM, Meddings L, Kaplan GG, Myers RP. Amoebic liver abscess in USA: a population-based study of incidence, temporal trends and mortality. Liver Int 2011; 31: 1191-1198.

149) Cosme A, Ojeda E, Zamarreo I, Bujanda L, Garmendia G, Echeverra MJ, Benavente J. Pyogenic versus amoebic liver abscesses: A comparative clinical study in a series of 58 patients. Revista Espaola De Enfermedades Dig 2010; 102: 90-95.

150) Polat P, Kantarci M, Alper F, Suma S, Koruyucu MB, Okur A. Hydatid Disease from Head to Toe1. Radiographics 2003; 23: 475-494.

151) Lopez-Bernus A, Belhassen-García M, Alonso-Sardón M, Carpio-Perez A, Velasco-Tirado V, Romero-Alegria Á, Muro A, Cordero-Sánchez M, Pardo-Lledias J. Surveillance of Human Echinococcosis in Castilla-Leon (Spain) between 2000-2012. Plos Neglect Trop D 2015; 9: e0004154.

152) Pedrosa I, Saíz A, Arrazola J, Ferreirós J, Pedrosa CS. Hydatid Disease: Radiologic and Pathologic Features and Complications1. Radiographics 2000; 20: 795-817.

153) Gharbi HA, Hassine W, Brauner MW, Dupuch K. Ultrasound examination of the hydatic liver. Radiology 1981; 139: 459-463.

154) WHO Informal Working Group. International classification of ultrasound images in cystic echinococcosis for application in clinical and field epidemiological settings. Acta Trop 2003; 85: 253-261.

155) Pedro MS, Semelka RC, Braga L. MR imaging of hepatic metastases. Magn Reson Imaging C 2002; 10: 15-29.

156) Sandrasegaran K, Rajesh A, Rydberg J, Rushing DA, Akisik FM, Henley JD. Gastrointestinal Stromal Tumors: Clinical, Radiologic, and Pathologic Features. Am J Roentgenol 2005; 184: 803-811.

157) Kanematsu M, Kondo H, Goshima S, Kato H, Tsuge U, Hirose Y, Kim MJ, Moriyama N. Imaging liver metastases: Review and update. Eur J Radiol 2006; 58: 217-228.

158) Warakaulle DR, Gleeson F. MDCT Appearance of Gastrointestinal Stromal Tumors After Therapy with Imatinib Mesylate. Am J Roentgenol 2006; 186: 510-515.

159) Lee MH, Katabathina VS, Lubner MG, Shah HU, Prasad SR, Matkowskyj KA, Pickhardt PJ. Mucin-producing Cystic Hepatobiliary Neoplasms: Updated Nomenclature and Clinical, Pathologic, and Imaging Features. Radiographics 2021; 41: 1592-1610.

160) Arnaoutakis DJ, Kim Y, Pulitano C, Zaydfudim V, Squires MH, Kooby D, Groeschl R, Alexandrescu S, Bauer TW, Bloomston M, Soares K, Marques H, Gamblin TC, Popescu I, Adams R, Nagorney D, Barroso E, Maithel SK, Crawford M, Sandroussi C, Marsh W, Pawlik TM. Management of Biliary Cystic Tumors. Ann Surg 2015; 261: 361-367.

161) Klompenhouwer AJ, Cate DWG ten, Willemssen FEJA, Bramer WM, Doukas M, Man RA de, Ijzermans JNM. The impact of imaging on the surgical management of biliary cystadenomas and cystadenocarcinomas; a systematic review. Hpb 2019; 21: 1257-1267.

162) Pech L, Favelier S, Falcoz MT, Loffroy R, Krause D, Cercueil JP. Imaging of Von Meyenburg complexes. Diagn Interv Imag 2016; 97: 401-409.

163) Torbenson MS. Hamartomas and malformations of the liver. Semin Diagn Pathol 2019; 36: 39-47.

164) Semelka RC, Hussain SM, Marcos HB, Woosley JT. Biliary Hamartomas: Solitary and Multiple Lesions Shown on Current MR Techniques Including Gadolinium Enhancement. J Magn Reson Imaging 1999; 10: 196-201.

165) Tohmé-Noun C, Cazals D, Noun R, Menassa L, Valla D, Vilgrain V. Multiple biliary hamartomas: magnetic resonance features with histopathologic correlation. Eur Radiol 2008; 18: 493-499.

166) Mamone G, Carollo V, Cortis K, Aquilina S, Liotta R, Miraglia R. Magnetic resonance imaging of fibropolycystic liver disease: the spectrum of ductal plate malformations. Abdom Radiol 2019; 44: 2156-2171.

167) Santos-Laso A, Izquierdo-Sánchez L, Lee-Law P, Perugorria M, Marzioni M, Marin J, Bujanda L, Banales J. New Advances in Polycystic Liver Diseases. Semin Liver Dis 2017; 37: 045-055.

168) Bazerbachi F, Haffar S, Sugihara T, Mounajjed TM, Takahashi N, Murad MH, Dayyeh BKA. Peribiliary cysts: a systematic review and proposal of a classification framework. Bmj Open Gastroenterology 2018; 5: e000204.

169) Danet IM, Semelka RC, Leonardou P, Braga L, Vaidean G, Woosley JT, Kanematsu M. Spectrum of MRI Appearances of Untreated Metastases of the Liver. Am J Roentgenol 2003; 181: 809-817.

170) Ozaki K, Higuchi S, Kimura H, Gabata T. Liver Metastases: Correlation between Imaging Features and Pathomolecular Environments. Radiographics 2022; 42: 1994-2013.

171) Horn SR, Stoltzfus KC, Lehrer EJ, Dawson LA, Tchelebi L, Gusani NJ, Sharma NK, Chen H, Trifiletti DM, Zaorsky NG. Epidemiology of liver metastases. Cancer Epidemiol 2020; 67: 101760.

172) Paget S. The distribution of secondary growths in cancer of the breast. 1889. Cancer Metastasis Rev 1989; 8: 98-101.

173) Brodt P. Role of the Microenvironment in Liver Metastasis: From Pre- to Prometastatic Niches. Clin Cancer Res 2016; 22: 5971-5982.

174) Wilkinson AL, Qurashi M, Shetty S. The Role of Sinusoidal Endothelial Cells in the Axis of Inflammation and Cancer Within the Liver. Front Physiol 2020; 11: 990.

175) BREEDIS C, YOUNG G. The blood supply of neoplasms in the liver. Am J Pathology 1954; 30: 969-977.

176) Namasivayam S, Martin DR, Saini S. Imaging of liver metastases: MRI. Cancer Imaging 2007; 7: 2-9.

177) Lincke T, Zech CJ. Liver metastases: Detection and staging. Eur J Radiol 2017; 97: 76-82.

178) Dam PJ van, Stok EP van der, Teuwen LA, Eynden GGV den, Illemann M, Frentzas S, Majeed AW, Eefsen RL, Braak RRJC van den, Lazaris A, Fernandez MC, Galjart B, Laerum OD, Rayes R, Grünhagen DJ, paer MV de, Sucaet Y, Mudhar HS, Schvimer M, Nyström H, Kockx M, Bird NC, Vidal-Vanaclocha F, Metrakos P, Simoneau E, Verhoef C, Dirix LY, Laere SV, Gao Z hua, Brodt P, Reynolds AR, Vermeulen PB. International consensus guidelines for scoring the histopathological growth patterns of liver metastasis. Brit J Cancer 2017; 117: 1427-1441.

179) Robertis RD, Geraci L, Tomaiuolo L, Bortoli L, Beleù A, Malleo G, D'Onofrio M. Liver metastases in pancreatic ductal adenocarcinoma: a predictive model based on CT texture analysis. Radiol Med 2022; 127: 1079-1084.

180) Oliveira RC, Alexandrino H, Cipriano MA, Tralhão JG. Liver Metastases and Histological Growth Patterns: Biological Behavior and Potential Clinical Implications—Another Path to Individualized Medicine? J Oncol 2019; 2019: 6280347.

181) Granata V, Fusco R, Muzio FD, Cutolo C, Setola SV, Dell'Aversana F, Grassi F, Belli A, Silvestro L, Ottaiano A, Nasti G, Avallone A, Flammia F, Miele V, Tatangelo F, Izzo F, Petrillo A. Radiomics and machine learning analysis based on magnetic resonance imaging in the assessment of liver mucinous colorectal metastases. Radiol Med 2022; 127: 763-772.

182) Semelka RC, Hussain SM, Marcos HB, Woosley JT. Perilesional Enhancement of Hepatic Metastases: Correlation between MR Imaging and Histopathologic Findings—Initial Observations. Radiology 2000; 215: 89-94.

183) Nielsen K, Rolff HC, Eefsen RL, Vainer B. The morphological growth patterns of colorectal liver metastases are prognostic for overall survival. Modern Pathol 2014; 27: 1641-1648.

184) Granata V, Fusco R, Muzio FD, Cutolo C, Setola SV, Grassi R, Grassi F, Ottaiano A, Nasti G, Tatangelo F, Pilone V, Miele V, Brunese MC, Izzo F, Petrillo A. Radiomics textural features by MR imaging to assess clinical outcomes following liver resection in colorectal liver metastases. Radiol Med 2022; 127: 461-470.

185) Yu JS, Rofsky NM. Hepatic Metastases: Perilesional Enhancement on Dynamic MRI. Am J Roentgenol 2006; 186: 1051-1058.

186) Paulatto L, Burgio MD, Sartoris R, Beaufrère A, Cauchy F, Paradis V, Vilgrain V, Ronot M. Colorectal liver metastases: radiopathological correlation. Insights Imaging 2020; 11: 99.

187) Granata V, Simonetti I, Fusco R, Setola SV, Izzo F, Scarpato L, Vanella V, Festino L, Simeone E, Ascierto PA, Petrillo A. Management of cutaneous melanoma: radiologists challenging and risk assessment. Radiol Med 2022; 127: 899-911.

188) Tang M, Li Y, Lin Z, Shen B, Huang M, Li ZP, Li X, Feng ST. Hepatic nodules with arterial phase hyperenhancement and washout on enhanced computed tomography/magnetic resonance imaging: how to avoid pitfalls. Abdom Radiol 2020; 45: 3730-3742.

189) Caruso D, Polici M, Rinzivillo M, Zerunian M, Nacci I, Marasco M, Magi L, Tarallo M, Gargiulo S, Iannicelli E, Annibale B, Laghi A, Panzuto F. CT-based radiomics for prediction of therapeutic response to Everolimus in metastatic neuroendocrine tumors. Radiol Med 2022; 127: 691-701.

190) Dromain C, Baere T de, Baudin E, Galline J, Ducreux M, Boige V, Duvillard P, Laplanche A, Caillet H, Lasser P, Schlumberger M, Sigal R. MR Imaging of Hepatic Metastases Caused by Neuroendocrine Tumors: Comparing Four Techniques. Am J Roentgenol 2003; 180: 121-128.

191) Benedetti G, Mori M, Panzeri MM, Barbera M, Palumbo D, Sini C, Muffatti F, Andreasi V, Steidler S, Doglioni C, Partelli S, Manzoni M, Falconi M, Fiorino C, Cobelli FD. CT-derived radiomic features to discriminate histologic characteristics of pancreatic neuroendocrine tumors. Radiol Med 2021; 126: 745-760.

192) Gulpinar B, Peker E, Kul M, Elhan AH, Halilioglu N. Liver metastases of neuroendocrine tumors: is it possible to diagnose different histologic subtypes depending on multiphasic CT features? Abdom Radiol 2019; 44: 2147-2155.

193) Palatresi D, Fedeli F, Danti G, Pasqualini E, Castiglione F, Messerini L, Massi D, Bettarini S, Tortoli P, Busoni S, Pradella S, Miele V. Correlation of CT radiomic features for GISTs with pathological classification and molecular subtypes: preliminary and monocentric experience. Radiol Med 2022; 127: 117-128.

194) Scoazec JY. Angiogenesis in Neuroendocrine Tumors: Therapeutic Applications. Neuroendocrinology 2013; 97: 45-56.

195) Jour G, Ivan D, Aung PP. Angiogenesis in melanoma: an update with a focus on current targeted therapies. J Clin Pathol 2016; 69: 472.

196) Papadakos SP, Tsagkaris C, Papadakis M, Papazoglou AS, Moysidis DV, Zografos CG, Theocharis S. Angiogenesis in gastrointestinal stromal tumors: From bench to bedside. World J Gastrointest Oncol 2022; 14: 1469-1477.

197) Danti G, Flammia F, Matteuzzi B, Cozzi D, Berti V, Grazzini G, Pradella S, Recchia L, Brunese L, Miele V. Gastrointestinal neuroendocrine neoplasms (GI-NENs): hot topics in morphological, functional, and prognostic imaging. Radiol Med 2021; 126: 1497-1507.

198) Inoue A, Ota S, Yamasaki M, Batsaikhan B, Furukawa A, Watanabe Y. Gastrointestinal stromal tumors: a comprehensive radiological review. Jpn J Radiol 2022; 40: 1105-1120.

199) Wang FH, Zheng HL, Li JT, Li P, Zheng CH, Chen QY, Huang CM, Xie JW. Prediction of recurrence-free survival and adjuvant therapy benefit in patients with gastrointestinal stromal tumors based on radiomics features. Radiol Med 2022; 127: 1085-1097.

200) Karaosmanoglu AD, Onur MR, Ozmen MN, Akata D, Karcaaltincaba M. Magnetic Resonance Imaging of Liver Metastasis. Seminars Ultrasound Ct Mri 2016; 37: 533-548.

201) Hardie AD, Egbert RE, Rissing MS. Improved differentiation between hepatic hemangioma and metastases on diffusion-weighted MRI by measurement of standard deviation of apparent diffusion coefficient. Clin Imag 2015; 39: 654-658.

202) Chiti G, Grazzini G, Flammia F, Matteuzzi B, Tortoli P, Bettarini S, Pasqualini E, Granata V, Busoni S, Messserini L, Pradella S, Massi D, Miele V. Gastroenteropancreatic neuroendocrine neoplasms (GEP-NENs): a radiomic model to predict tumor grade. Radiol Med 2022; 127: 928-938.

203) KANEMATSU M, GOSHIMA S, WATANABE H, KONDO H, KAWADA H, NODA Y, MORIYAMA N. Diffusion/Perfusion MR Imaging of the Liver: Practice, Challenges, and Future. Magn Reson Med Sci 2012; 11: 151-161.

204) Löwenthal D, Zeile M, Lim WY, Wybranski C, Fischbach F, Wieners G, Pech M, Kropf S, Ricke J, Dudeck O. Detection and characterisation of focal liver lesions in colorectal carcinoma patients: comparison of diffusion-weighted and Gd-EOB-DTPA enhanced MR imaging. Eur Radiol 2011; 21: 832-840.

205) Leon M, Chavez L, Surani S. Hepatic hemangioma: What internists need to know. World J Gastroentero 2020; 26: 11-20.

206) Caseiro-Alves F, Brito J, Araujo AE, Belo-Soares P, Rodrigues H, Cipriano A, Sousa D, Mathieu D. Liver haemangioma: common and uncommon findings and how to improve the differential diagnosis. Eur Radiol 2007; 17: 1544-1554.

207) Mamone G, Piazza AD, Carollo V, Cannataci C, Cortis K, Bartolotta TV, Miraglia R. Imaging of hepatic hemangioma: from A to Z. Abdom Radiol 2020; 45: 672-691.

208) Klotz T, Montoriol PF, Ines DD, Petitcolin V, Joubert-Zakeyh J, Garcier JM. Hepatic haemangioma: Common and uncommon imaging features. Diagn Interv Imag 2013; 94: 849-859.

209) Doyle DJ, Khalili K, Guindi M, Atri M. Imaging Features of Sclerosed Hemangioma. Am J Roentgenol 2007; 189: 67-72.

210) Makhlouf HR, Ishak KG. Sclerosed hemangioma and sclerosing cavernous hemangioma of the liver: a comparative clinicopathologic and immunohistochemical study with emphasis on the role of mast cells in their histogenesis. Liver 2002; 22: 70-78.

211) Brancatelli G, Federle MP, Blachar A, Grazioli L. Hemangioma in the Cirrhotic Liver: Diagnosis and Natural History. Radiology 2001; 219: 69-74.

212) Nguyen BN, Fléjou JF, Terris B, Belghiti J, Degott C. Focal Nodular Hyperplasia of the Liver. Am J Surg Pathology 1999; 23: 1441.

213) Wanless IR. The pathogenesis of focal nodular hyperplasia of the liver. J Gastroen Hepatol 2004; 19: S342-S343.

214) LeGout JD, Bolan CW, Bowman AW, Caserta MP, Chen FK, Cox KL, Sanyal R, Toskich BB, Lewis JT, Alexander LF. Focal Nodular Hyperplasia and Focal Nodular Hyperplasia–like Lesions. Radiographics 2022; 42: 1043-1061.

215) Mortelé KJ, Praet M, Vlierberghe HV, Kunnen M, Ros PR. CT and MR Imaging Findings in Focal Nodular Hyperplasia of the Liver: Radiologic—Pathologic Correlation. Am J Roentgenol 2000; 175: 687-692.

216) Dohan A, Soyer P, Guerrache Y, Hoeffel C, Gavini JP, Kaci R, Boudiaf M. Focal Nodular Hyperplasia of the Liver: diffusion-weighted magnetic resonance imaging characteristics using high b values. J Comput Assist Tomogr 2014; 38: 96-104;

217) Miller FH, Hammond N, Siddiqi AJ, Shroff S, Khatri G, Wang Y, Merrick LB, Nikolaidis P. Utility of diffusion-weighted MRI in distinguishing benign and malignant hepatic lesions. J Magn Reson Imaging 2010; 32: 138-147.

218) Grazioli L, Bondioni MP, Haradome H, Motosugi U, Tinti R, Frittoli B, Gambarini S, Donato F, Colagrande S. Hepatocellular Adenoma and Focal Nodular Hyperplasia: Value of Gadoxetic Acid–enhanced MR Imaging in Differential Diagnosis. Radiology Published online 2012.

219) Grazioli L, Morana G, Kirchin MA, Schneider G. Accurate Differentiation of Focal Nodular Hyperplasia from Hepatic Adenoma at Gadobenate Dimeglumine–enhanced MR Imaging: Prospective Study. Radiology 2005; 236: 166-177.

220) Kessel CS van, Boer E de, Kate FJW ten, Brosens LAA, Veldhuis WB, Leeuwen MS van. Focal nodular hyperplasia: hepatobiliary enhancement patterns on gadoxetic-acid contrast-enhanced MRI. Abdom Imaging 2013; 38: 490-501.

221) Fujita N, Nishie A, Asayama Y, Ishigami K, Ushijima Y, Kakihara D, Nakayama T, Morita K, Ishimatsu K, Honda H. Hyperintense Liver Masses at Hepatobiliary Phase Gadoxetic Acid–enhanced MRI: Imaging Appearances and Clinical Importance. Radiographics 2020; 40: 72-94.

222) European Association for the Study of the Liver (EASL). EASL Clinical Practice Guidelines on the management of benign liver tumours. J Hepatol 2016; 65: 386-398.

223) Shaked O, Siegelman ES, Olthoff K, Reddy KR. Biologic and Clinical Features of Benign Solid and Cystic Lesions of the Liver. Clin Gastroenterol H 2011; 9: 547-562.e4.

224) Stoot JHMB, Coelen RJS, Jong MCD, Dejong CHC. Malignant transformation of hepatocellular adenomas into hepatocellular carcinomas: a systematic review including more than 1600 adenoma cases. Hpb 2010; 12: 509-522.

225) Myers L, Ahn J. Focal Nodular Hyperplasia and Hepatic Adenoma Evaluation and Management. Clin Liver Dis 2020; 24: 389-403.

226) Nault JC, Couchy G, Balabaud C, Morcrette G, Caruso S, Blanc JF, Bacq Y, Calderaro J, Paradis V, Ramos J, Scoazec JY, Gnemmi V, Sturm N, Guettier C, Fabre M, Savier E, Chiche L, Labrune P, Selves J, Wendum D, Pilati C, Laurent A, Muret AD, Bail BL, Rebouissou S, Imbeaud S, Investigators G, Laurent C, Saric J, Frulio N, Castain C, Dujardin F, Benchellal Z, Bourlier P, Azoulay D, Luciani A, Pageaux GP, Fabre JM, Vilgrain V, Belghiti J, Bancel B, Boleslawski E, Letoublon C, Vaillant JC, Prévôt S, Castaing D, Jacquemin E, Peron JM, Quaglia A, Paye F, Terraciano L, Mazzaferro V, Paul MCS, Terris B, Bioulac-Sage P, Letouzé E, Zucman-Rossi J. Molecular Classification of Hepatocellular Adenoma Associates With Risk Factors, Bleeding, and Malignant Transformation. Gastroenterology 2017; 152: 880-894.e6.

227) Tse JR, Felker ER, Cao JJ, Naini BV, Liang T, Lu DSK, Raman SS. Hepatocellular Adenoma Subtypes Based on 2017 Classification System: Exploratory Study of Gadoxetate Disodium-Enhanced MRI Features With Proposal of a Diagnostic Algorithm. AJR Am J Roentgenol 2023; 220: 539-550.

228) Guo Y, Li W, Cai W, Zhang Y, Fang Y, Hong G. Diagnostic Value of Gadoxetic Acid-Enhanced MR Imaging to Distinguish HCA and Its Subtype from FNH: A Systematic Review. Int J Med Sci 2017; 14: 668-674.

229) McInnes MDF, Hibbert RM, Inácio JR, Schieda N. Focal Nodular Hyperplasia and Hepatocellular Adenoma: Accuracy of Gadoxetic Acid–enhanced MR Imaging—A Systematic Review. Radiology 2015; 277: 413-423.

230) Bilreiro C, Soler JC, Ayuso JR, Caseiro-Alves F, Ayuso C. Diagnostic value of morphological enhancement patterns in the hepatobiliary phase of gadoxetic acid-enhanced MRI to distinguish focal nodular hyperplasia from hepatocellular adenoma. Radiol Med 2021; 126: 1379-1387.

231) Moosavi B, Shenoy-Bhangle AS, Tsai LL, Reuf R, Mortele KJ. MRI characterization of focal liver lesions in non-cirrhotic patients: assessment of added value of gadoxetic acid-enhanced hepatobiliary phase imaging. Insights Imaging 2020; 11: 101.

232) Mamone G, Piazza AD, Carollo V, Crinò F, Vella S, Cortis K, Miraglia R. Imaging of primary malignant tumors in non-cirrhotic liver. Diagn Interv Imag 2020; 101: 519-535.

233) Khan SA, Thomas HC, Davidson BR, Taylor-Robinson SD. Cholangiocarcinoma. Lancet 2005; 366: 1303-1314.

234) Chung YE, Kim MJ, Park YN, Choi JY, Pyo JY, Kim YC, Cho HJ, Kim KA, Choi SY. Varying Appearances of Cholangiocarcinoma: Radiologic-Pathologic Correlation. Radiographics 2009; 29: 683-700.

235) Joo I, Lee JM, Yoon JH. Imaging Diagnosis of Intrahepatic and Perihilar Cholangiocarcinoma: Recent Advances and Challenges. Radiology 2018; 288: 7-13.

236) Sempoux1 C, Jibara2 G, Ward3 S, Fan3 C, Qin3 L, Roayaie2 S, Fiel3 MI, Schwartz2 M, Thung3 S. Intrahepatic Cholangiocarcinoma: New Insights in Pathology. Semin Liver Dis 2011; 31: 049-060.

237) Granata V, Grassi R, Fusco R, Setola SV, Belli A, Ottaiano A, Nasti G, Porta ML, Danti G, Cappabianca S, Cutolo C, Petrillo A, Izzo F. Intrahepatic cholangiocarcinoma and its differential diagnosis at MRI: how radiologist should assess MR features. Radiol Med 2021; 126: 1584-1600.

238) Kim SA, Lee JM, Lee KB, Kim SH, Yoon SH, Han JK, Choi BI. Intrahepatic Mass-forming Cholangiocarcinomas: Enhancement Patterns at Multiphasic CT, with Special Emphasis on Arterial Enhancement Pattern—Correlation with Clinicopathologic Findings. Radiology 2011; 260: 148-157.

239) Bozkurt M, Eldem G, Bozbulut UB, Bozkurt MF, Kılıçkap S, Peynircioğlu B, Çil B, Ergün EL, Volkan-Salanci B. Factors affecting the response to Y-90 microsphere therapy in the cholangiocarcinoma patients. Radiol Med 2021; 126: 323-333.

240) Kim R, Lee JM, Shin CI, Lee ES, Yoon JH, Joo I, Kim SH, Hwang I, Han JK, Choi BI. Differentiation of intrahepatic mass-forming cholangiocarcinoma from hepatocellular carcinoma on gadoxetic acid-enhanced liver MR imaging. Eur Radiol 2016; 26: 1808-1817.

241) Hu J, Liu W, Xie S, Li M, Wang K, Li W. Abdominal perivascular epithelioid cell tumor (PEComa) without visible fat: a clinicopathologic and radiological analysis of 16 cases. Radiol Med 2021; 126: 189-199.

242) Ginès P, Krag A, Abraldes JG, Solà E, Fabrellas N, Kamath PS. Liver cirrhosis. Lancet 2021; 398: 1359-1376.

243) Torres WE, Whitmire LF, Gedgaudas-McClees K, Bernardino ME. Computed Tomography of Hepatic Morphologic Changes in Cirrhosis of the Liver. J Comput Assist Tomo 1986; 10: 47-50.

244) Ohtomo K, Baron RL, Dodd GD, Federle MP, Miller WJ, Campbell WL, Confer SR, Weber KM. Confluent hepatic fibrosis in advanced cirrhosis: appearance at CT. Radiology 1993; 188: 31-35.

245) Ito K, Mitchell DG, Gabata T. Enlargement of hilar periportal space: A sign of early cirrhosis at MR imaging. J Magn Reson Imaging 2000; 11: 136-140.

246) Ito K, Mitchell DG, Gabata T, Hussain SM. Expanded Gallbladder Fossa: Simple MR Imaging Sign of Cirrhosis. Radiology 1999; 211: 723-726.

247) Hyodo R, Takehara Y, Naganawa S. 4D Flow MRI in the portal venous system: imaging and analysis methods, and clinical applications. Radiol Med 2022; 127: 1181-1198.

248) Annet L, Materne R, Danse E, Jamart J, Horsmans Y, Beers BEV. Hepatic Flow Parameters Measured with MR Imaging and Doppler US: Correlations with Degree of Cirrhosis and Portal Hypertension. Radiology 2003; 229: 409-414.

249) Scheinfeld MH, Bilali A, Koenigsberg M. Understanding the Spectral Doppler Waveform of the Hepatic Veins in Health and Disease. Radiographics 2009; 29: 2081-2098.

250) Cannataci C, Cimo' B, Mamone G, Tuzzolino F, D'Amico M, Cortis K, Maruzzelli L, Miraglia R. Portal vein puncture-related complications during transjugular intrahepatic portosystemic shunt creation: Colapinto needle set vs Rösch-Uchida needle set. Radiol Med 2021; 126: 1487-1495.

251) McNaughton DA, Abu-Yousef MM. Doppler US of the Liver Made Simple1. Radiographics 2011; 31: 161-188.

252) Dyvorne HA, Knight-Greenfield A, Besa C, Cooper N, Garcia-Flores J, Schiano TD, Markl M, Taouli B. Quantification of Hepatic Blood Flow Using a High-Resolution Phase-Contrast MRI Sequence With Compressed Sensing Acceleration. Am J Roentgenol 2015; 204: 510-518.

253) Lee DH, Lee ES, Lee JY, Bae JS, Kim H, Lee KB, Yu SJ, Cho EJ, Lee JH, Cho YY, Han JK, Choi BI. Two-Dimensional-Shear Wave Elastography with a Propagation Map: Prospective Evaluation of Liver Fibrosis Using Histopathology as the Reference Standard. Korean J Radiol 2020; 21: 1317-1325.

254) Argalia G, Tarantino G, Ventura C, Campioni D, Tagliati C, Guardati P, Kostandini A, Marzioni M, Giuseppetti GM, Giovagnoni A. Shear wave elastography and transient elastography in HCV patients after direct-acting antivirals. Radiol Med 2021; 126: 894-899.

255) Guglielmo FF, Venkatesh SK, Mitchell DG. Liver MR Elastography Technique and Image Interpretation: Pearls and Pitfalls. Radiographics 2019; 39: 1983-2002.

256) Dana J, Venkatasamy A, Saviano A, Lupberger J, Hoshida Y, Vilgrain V, Nahon P, Reinhold C, Gallix B, Baumert TF. Conventional and artificial intelligence-based imaging for biomarker discovery in chronic liver disease. Hepatol Int 2022; 16: 509-522.

257) Vicini S, Bortolotto C, Rengo M, Ballerini D, Bellini D, Carbone I, Preda L, Laghi A, Coppola F, Faggioni L. A narrative review on current imaging applications of artificial intelligence and radiomics in oncology: focus on the three most common cancers. Radiol Med 2022; 127: 819-836.

258) Wu L, Ning B, Yang J, Chen Y, Zhang C, Yan Y. Diagnosis of Liver Cirrhosis and Liver Fibrosis by Artificial Intelligence Algorithm-Based Multislice Spiral Computed Tomography. Comput Math Method M 2022; 2022: 1217003.

259) Elkassem AA, Allen BC, Lirette ST, Cox KL, Remer EM, Pickhardt PJ, Lubner MG, Sirlin CB, Dondlinger T, Schmainda M, Jacobus RB, Severino PE, Smith AD. Multiinstitutional Evaluation of the Liver Surface Nodularity Score on CT for Staging Liver Fibrosis and Predicting Liver-Related Events in Patients With Hepatitis C. Am J Roentgenol 2022; 218: 833-845.

260) Cicero G, Mazziotti S, Silipigni S, Blandino A, Cantisani V, Pergolizzi S, D'Angelo T, Stagno A, Maimone S, Squadrito G, Ascenti G. Dual-energy CT quantification of fractional extracellular space in cirrhotic patients: comparison between early and delayed equilibrium phases and correlation with oesophageal varices. Radiol Med 2021; 126: 761-767.

261) Fujita S, Sano K, Cruz G, Fukumura Y, Kawasaki H, Fukunaga I, Morita Y, Yoneyama M, Kamagata K, Abe O, Ikejima K, Botnar RM, Prieto C, Aoki S. MR Fingerprinting for Liver Tissue Characterization: A Histopathologic Correlation Study. Radiology Published online 2022: 220736.

262) Ledda RE, Milanese G, Cademartiri F, Maffei E, Benedetti G, Goldoni M, Silva M, Sverzellati N. Association of hepatic steatosis with epicardial fat volume and coronary artery disease in symptomatic patients. Radiol Med 2021; 126: 652-660.

263) Bannas P, Kramer H, Hernando D, Agni R, Cunningham AM, Mandal R, Motosugi U, Sharma SD, Rio AM del, Fernandez L, Reeder SB. Quantitative magnetic resonance imaging of hepatic steatosis: Validation in ex vivo human livers. Hepatology 2015; 62: 1444-1455.

264) Burgio MD, Ronot M, Reizine E, Rautou PE, Castera L, Paradis V, Garteiser P, Beers BV, Vilgrain V. Quantification of hepatic steatosis with ultrasound: promising role of attenuation imaging coefficient in a biopsy-proven cohort. Eur Radiol 2020; 30: 2293-2301.

265) Kramer H, Pickhardt PJ, Kliewer MA, Hernando D, Chen GH, Zagzebski JA, Reeder SB. Accuracy of Liver Fat Quantification With Advanced CT, MRI, and Ultrasound Techniques: Prospective Comparison With MR Spectroscopy. AJR American journal of roentgenology 2017; 208: 92-100.

266) Argalia G, Ventura C, Tosi N, Campioni D, Tagliati C, Tufillaro M, Cucco M, Baroni GS, Giovagnoni A. Comparison of point shear wave elastography and transient elastography in the evaluation of patients with NAFLD. Radiol Med 2022; 127: 571-576.

267) European Association for the Study of the Liver. EASL Clinical Practice Guidelines: Liver transplantation. J Hepatol 2016; 64: 433-485.

268) Li J, Cao B, Bi X, Chen W, Wang L, Du Z, Zhang X, Yu X. Evaluation of liver function in patients with chronic hepatitis B using Gd-EOB-DTPA-enhanced T1 mapping at different acquisition time points: a feasibility study. Radiol Med 2021; 126: 1149-1158.

269) Dhaliwal A, Armstrong MJ. Sarcopenia in cirrhosis: A practical overview. Clin Med 2020; 20: 489-492.

270) Tagliafico AS, Bignotti B, Torri L, Rossi F. Sarcopenia: how to measure, when and why. Radiol Med 2022; 127: 228-237.

271) Brody RI, Theise ND. An inflammatory proposal for hepatocarcinogenesis. Hepatology 2012; 56: 382-384.

272) Stefanini M, Simonetti G. Interventional Magnetic Resonance Imaging Suite (IMRIS): How to build and how to use. Radiol Med 2022; 127: 1063-1067.

273) Park YN. Update on Precursor and Early Lesions of Hepatocellular Carcinomas. Arch Pathol Lab Med 2011; 135: 704-715.

274) Coleman WB. Mechanisms of Human Hepatocarcinogenesis. Curr Mol Med 2003; 3: 573-588.

275) Park YN, Kim MJ. Hepatocarcinogenesis: imaging-pathologic correlation. Abdom Imaging 2011; 36: 232-243.

276) Sakamoto M. Pathology of early hepatocellular carcinoma. Hepatol Res 2007; 37: S135-S138.

277) Kojiro M. Histopathology of liver cancers. Best Pract Res Clin Gastroenterology 2005; 19: 39-62.

278) Park YN, Yang CP, Fernandez GJ, Cubukcu O, Thung SN, Theise ND. Neoangiogenesis and Sinusoidal "Capillarization" in Dysplastic Nodules of the Liver. Am J Surg Pathology 1998; 22: 656-662.

279) Kitao A, Zen Y, Matsui O, Gabata T, Nakanuma Y. Hepatocarcinogenesis: Multistep Changes of Drainage Vessels at CT during Arterial Portography and Hepatic Arteriography—Radiologic-Pathologic Correlation. Radiology 2009; 252: 605-614.

280) Matsui O, Kobayashi S, Sanada J, Kouda W, Ryu Y, Kozaka K, Kitao A, Nakamura K, Gabata T. Hepatocelluar nodules in liver cirrhosis: hemodynamic evaluation (angiography-assisted CT) with special reference to multi-step hepatocarcinogenesis. Abdom Imaging 2011; 36: 264-272.

281) Kitao A, Matsui O, Yoneda N, Kozaka K, Shinmura R, Koda W, Kobayashi S, Gabata T, Zen Y, Yamashita T, Kaneko S, Nakanuma Y. The uptake transporter OATP8 expression decreases during multistep hepatocarcinogenesis: correlation with gadoxetic acid enhanced MR imaging. Eur Radiol 2011; 21: 2056-2066.

282) Nakamura Y, Higaki T, Honda Y, Tatsugami F, Tani C, Fukumoto W, Narita K, Kondo S, Akagi M, Awai K. Advanced CT techniques for assessing hepatocellular carcinoma. Radiol Med 2021; 126: 925-935.

283) Choi JY, Lee JM, Sirlin CB. CT and MR Imaging Diagnosis and Staging of Hepatocellular Carcinoma: Part I. Development, Growth, and Spread: Key Pathologic and Imaging Aspects. Radiology 2014; 272: 635-654.

284) Choi JY, Lee JM, Sirlin CB. CT and MR Imaging Diagnosis and Staging of Hepatocellular Carcinoma: Part II. Extracellular Agents, Hepatobiliary Agents, and Ancillary Imaging Features. Radiology 2014; 273: 30-50.

285) Seeff LB, Everson GT, Morgan TR, Curto TM, Lee WM, Ghany MG, Shiffman ML, Fontana RJ, Bisceglie AMD, Bonkovsky HL, Dienstag JL, Group HT. Complication Rate of Percutaneous Liver Biopsies Among Persons With Advanced Chronic Liver Disease in the HALT-C Trial. Clin Gastroenterol H 2010; 8: 877-883.

286) Gore RM, Newmark GM, Thakrar KH, Mehta UK, Berlin JW. Hepatic Incidentalomas. Radiol Clin N Am 2011; 49: 291-322.

287) Scialpi M, Moschini TO, Filippis GD. PET/contrast-enhanced CT in oncology: "to do, or not to do, that is the question." Radiol Med 2022; 127: 925-927.

288) American College of Radiology Committee on LI-RADS® (Liver). Chapter 11. Management. LI-RADS® v2018. CT/MRI Manual. Published 2018. Accessed December 21, 2022. Available at: https://www.acr.org/-/media/ACR/Files/Clinical-Resources/LIRADS/Chapter-11-Management.pdf?la=en&;hash=767E90E7CED2AA0B-8D5AE20F1B1ED610.

289) Granata V, Fusco R, Venanzio Setola S, Barretta ML, Iasevoli DMA, Palaia R, Belli A, Patrone R, Tatangelo F, Grazzini G, Grassi R, Grassi F, Grassi R, Anselmo A, Izzo F, Petrillo A. Diagnostic performance of LI-RADS in adult patients with rare hepatic tumors. Eur Rev Med Pharmacol Sci 2022; 26: 399-414.